TEORIJSKA I PRIMENJENA MEHANIKA 18, pp 41-80, 1992, UDK 539.31+531/534

# APPLICATION OF THE COMPLEX VARIABLE FUNCTION TO CRACK PROBLEM IN THE PIEZOELECTRIC MATERIAL

*K. Hedrih, Lj. Perić*

(Received 07.05.1992.; in revised form 15.06.1993.)

## 0. Introduction

It is known that the crytical electric polarization caused by its stretching or compression is known as the "piezoelectric effect". This process is characterized by the appearance of electrostatic charges on the piezoelectric material surface whereas the electric polarization happens within it.

When an electric charge is brought upon the parallel opposite surfaces of the piezoelectric material then the mechanical deformation is formed which is proportional to the electric field magnitude. This phenomenon is known as the "inverse piezoelectric effect".

Since the piezoelectric effect appears due to the mutual effects of the mechanical stress and the electric field it is necessary to examine the piezoelectric material electromechanical state through a coresponding coupling of its electric and mechanical fields.

Although the piezoelectric materials have been used in many electromechanical devices for many decades there are only a few theoretical papers published dealing with their mechanical defect. Among the papers dealing with this problem and on the basis of our subjective knowledge we point out the paper of Parton V. Z. (1976) and Deeg W. F. (1980) on the fracture problem in piezoelectric materials. Pak Y. E. (1990) described the crack behaviour within a piezoelectric material as well as its effect on the fracture of a piezoelectric material itself. He also showed that the crack growth can be hindered or enhanced depending on the magnitude and sense of the applied electric load. The conclusions reached by Pak in the given References are in agreement with those reached by Deeg W. F. (1980) and they refer to the consideration of the fracture problem of a piezoelectric material in-plane by the divided dislocation method. We also point out the most recent papers by Sosa H. A. and Pak Y. E. (1988) on the space analysis of the crack effect upon the piezoelectric material behaviour as well as the papers of Frieman S. W. (1986) and Pak Y. E. (1980).

In our papers [12] and [13] of 1992 we determined the analytical approximations for the mechanical stress tensor components, for the relative deformation tensors and for the piezoelectric stress components for the case of a plane deformation of a

crack for the modes I and II and for the case of a space deformation for the mode III and we showed a graphical representation of the parameters distribution of the electromechanical state of a piezoelectric material around the crack tip.

In this paper we examine the role of a semi-infinite crack which is found as a defect within a piezoelectric medium. The examination is based upon the application of the linear elasticity theory for the case of the material shear along the crack surface for the case of the vector displacement in and out of the crack referential plane. In this paper we introduce the stress function $\Phi(r,\theta)$ as well as the function $\Phi_E(r,\theta)$ of the electric potential.

We apply the method of the complex variable analytical functions which are assumed to be in the form of the graded infinite orders. The paper's aim is to determine the analytical expressions and the graphical representation of the components of the mechanical and electric stresses tensors as well as the relative deformation tensor components and the displacement vector around the crack tip. These studies comprise all three basic forms of the crack deformation, that is, the modes I, II and III.

## 1. Problem statement

The separating crack surfaces in a piezoelectric material present unloaded boundaries of a stressed body and therefore the stress distribution at the points around tha crack tip depends on the form of the fracture surface generation. The achievements of the linear elastic fracture mechanics accept the assumption about three basic forms (modes) of the crack deformation which we will accept as well. The deformation plane state is characterized by the two basic forms of the fracture surface generation which we have mentioned in our paper [12] whereas the crack deformation space state has been studied in our paper [13]. Here our study is directed towards the same tascs as in the quoted papers but this time the method applied is the one of the complex variable analytical functions.

The sketches 1, 2 and 3 show the characteristic shapes of the crack deformations by the mode I, II and III with the corresponding assumed possible coordinates of the displacement vectors of the points around the crack.

The modes I and II correspond to the assumption about the plane deformation in the crack referential plane.

The mode III corresponds to the assumption about the shear of the crack points along the crack surface by the crack points appearance perpendicularly to the referential plane. This means that the crack mode III is defined by one crack surface displacement along the other one's front, so that the points which were in the same referential plane perpendicular to the crack surface before the crack deformation (generation) are not in it after the crack deformation (generation). The parametar $\mathcal{R}_{III}$ is a stress intensity factor for the respective mode III.

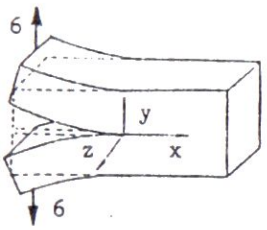


$u = u(r,\theta)$
$v = v(r,\theta)$
$w = 0$

Sketch No. 1

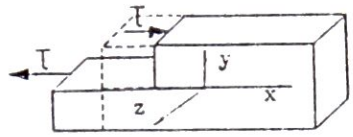


$u = u(r,\theta)$
$v = v(r,\theta)$
$w = 0$

Sketch No. 2

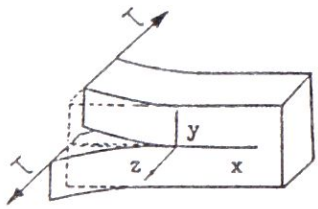


$u = 0$
$v = 0$
$w = w(r,\theta)$

Sketch No. 3

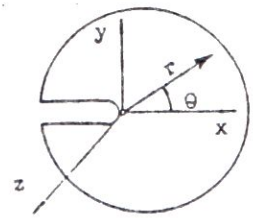


Sketch No. 4

According to the elastic linear fracture theory and for the case of the deformation space state the crack front can be accepted as a curve in the space whose every point contains all the three deformation modes so that we can accept the assumption that the mechanical stress components are of the form:

$$\sigma_{ij}(r,\theta,z) = \frac{1}{\sqrt{2\pi r}}[\mathcal{R}_I(z)\sigma_{ij}^I(r,\theta) + \mathcal{R}_{II}(z)\sigma_{ij}^{II}(r,\theta) + \mathcal{R}_{III}(z)\sigma_{ij}^{III}(r,\theta)].$$

The coefficients $\mathcal{R}_I$, $\mathcal{R}_{II}$ and $\mathcal{R}_{III}$ are the stress intensity factors for the respective modes. The recommendations for determining the stress intensity factors can be found in the books by Tada H. (1973) and Murakami Y. (1987).

Our study will be focused upon piezoelectric ceramics with a hexagonal crystal system of the class $6_{mm}$ which is characterized by five elasticity tensor constants $c_{ijkl}$, three piezoelectricity constants $e_{ijk}$ and two dielectric constants $b_{ik}$. This kind of piezoelectric medium is most present in ultrasonic transformers it possesses a great efficiency of conversion of electric energy into mechanical and vica versa.

The sketch No. 4 shows a crack in the referential plane perpendicular to the crack front with a polar coordinates system in which the crack orientation is denoted in the direction of the axis $Oz$, whereas the axis $Oy$ is perpendicular to the basic crack plane. Let's assume that the crack surface appearance is without any surface micro defects.

## 2. Governing equations

The basic equations adopted for a piezoelectric material which we will use and which can be found in the given References are:

For *Electric enthalpy*

$$\mathcal{H}(\varepsilon_{ij}, E_i) = \frac{1}{2}c_{ijkl}\varepsilon_{ij}\varepsilon_{kl} - \frac{1}{2}\delta_{ij}E_iE_j - e_{ikl}\varepsilon_{kl}E_i, \tag{1}$$

for the *specific deformation (strain) tensor*

$$\varepsilon_{ij} = \frac{1}{2}(u_{i,j} + u_{j,i}), \tag{2}$$

for the *stress tensor*

$$\sigma_{ij} = \frac{\partial \mathcal{H}}{\partial \varepsilon_{ij}} = c_{ijkl}\varepsilon_{kl} - e_{kij}E_k, \tag{3}$$

for the *piezoelectric stress*

$$\mathcal{D}_i = -\frac{\partial \mathcal{H}}{\partial E_1} = e_{ikl}\varepsilon_{kl} + \delta_{ik}E_k, \tag{4}$$

for the *electric field vector components*

$$E_i = -\Phi_{E,i}. \tag{5}$$

In absence of the volume forces and free electric charges the equilibrium equations are:

$$\sigma_{ij,j} = 0, \tag{6}$$

$$\mathcal{D}_{i,i} = 0, \tag{7}$$

where $\sigma_{ij}$ are the mechanical stress tensor coordinates, $\mathcal{D}_i$ are the piezoelectric stress coordinates, $E_k$ are the electric field components, $\Phi_E$ is an electric potential and $\varepsilon_{ij}$ are the relative deformation tensor coordinates.

The extended Hooke's Law for a given piezoelectric material of a hexagonal crystal system of the crystal class $C_{6V}$ is of the form

$$\begin{pmatrix} \sigma_r \\ \sigma_\theta \\ \sigma_z \\ \tau_{\theta z} \\ \tau_{rz} \\ \tau_{r\theta} \end{pmatrix} = \begin{pmatrix} c_{11} & c_{12} & c_{13} & 0 & 0 & 0 \\ c_{12} & c_{11} & c_{13} & 0 & 0 & 0 \\ c_{13} & c_{13} & c_{33} & 0 & 0 & 0 \\ 0 & 0 & 0 & c_{44} & 0 & 0 \\ 0 & 0 & 0 & 0 & c_{44} & 0 \\ 0 & 0 & 0 & 0 & 0 & \frac{c_{11}-c_{12}}{2} \end{pmatrix} \begin{pmatrix} \varepsilon_r \\ \varepsilon_\theta \\ \varepsilon_z \\ 2\varepsilon_{\theta z} \\ 2\varepsilon_{rz} \\ 2\varepsilon_{r\theta} \end{pmatrix} - \begin{pmatrix} 0 & 0 & e_{31} \\ 0 & 0 & e_{31} \\ 0 & 0 & e_{33} \\ 0 & e_{15} & 0 \\ e_{15} & 0 & 0 \\ 0 & 0 & 0 \end{pmatrix} \begin{pmatrix} E_r \\ E_\theta \\ E_z \end{pmatrix} \tag{8}$$

and it gives the relation between the mechanical stress tensor coordinates, the strain (specific deformation) tensor and the electric field vector coordinates. For the piezoelectric stress vector we can write the following relation:

$$\begin{pmatrix} \mathcal{D}_r \\ \mathcal{D}_\theta \\ \mathcal{D}_z \end{pmatrix} = \begin{pmatrix} 0 & 0 & 0 & 0 & e_{15} & 0 \\ 0 & 0 & 0 & e_{15} & 0 & 0 \\ e_{31} & e_{31} & e_{33} & 0 & 0 & 0 \end{pmatrix} \begin{pmatrix} \varepsilon_r \\ \varepsilon_\theta \\ \varepsilon_z \\ 2\varepsilon_{\theta z} \\ 2\varepsilon_{rz} \\ 2\varepsilon_{r\theta} \end{pmatrix} + \begin{pmatrix} \delta_{11} & 0 & 0 \\ 0 & \delta_{11} & 0 \\ 0 & 0 & \delta_{33} \end{pmatrix} \begin{pmatrix} E_r \\ E_\theta \\ E_z \end{pmatrix}.$$

## 3. Plane deformation state

The plane deformation state is defined with the displacement field

$$u = u(r,\theta), \quad v = v(r,\theta), \quad w = 0, \tag{10}$$

as well as the electric field

$$E_r = 0, \quad E_\theta = 0, \quad E_z = E_z(r,\theta). \tag{11}$$

The relative deformation (strain) tensor matrix elements are expressed via the coordinates $u$ and $v$ of the displacement vector and they are

$$\left.\begin{aligned} &\varepsilon_r = \frac{\partial u}{\partial r}, \qquad \varepsilon_\theta = \frac{1}{r}\left(\frac{\partial v}{\partial \theta} + u\right), \qquad \varepsilon_z = 0 \\ &\varepsilon_{r\theta} = \frac{1}{2}\left[\frac{1}{r}\left(\frac{\partial u}{\partial \theta} - v\right) + \frac{\partial v}{\partial r}\right], \qquad \varepsilon_{rz} = 0, \qquad \varepsilon_{\theta z} = 0. \end{aligned}\right\} \tag{12}$$

The mechanical stress tensor matrix elements are

$$\left.\begin{aligned} &\sigma_r = c_{11}\frac{\partial u}{\partial r} + c_{12}\frac{1}{r}\left(\frac{\partial v}{\partial \theta} + u\right), \quad \sigma_\theta = c_{12}\frac{\partial u}{\partial r} + c_{11}\frac{1}{r}\left(\frac{\partial v}{\partial \theta} + u\right), \\ &\sigma_z = c_{13}\frac{\partial u}{\partial r} + c_{13}\frac{1}{r}\left(\frac{\partial v}{\partial \theta} + u\right), \\ &\tau_{rz} = \frac{1}{2}(c_{11} - c_{12})\left[\frac{1}{r}\left(\frac{\partial u}{\partial \theta} - v\right) + \frac{\partial v}{\partial r}\right], \quad \tau_{rz} = 0, \quad \tau_{\theta z} = 0. \end{aligned}\right\} \tag{13}$$

The piezoelectric stress components are

$$\mathcal{D}_r = 0, \quad \mathcal{D}_\theta = 0, \quad \mathcal{D}_z = e_{31}\frac{\partial u}{\partial r} + e_{31}\frac{1}{r}\left(\frac{\partial v}{\partial \theta} + u\right). \tag{14}$$

The Belltramy conditions of the stress compatibility (the Morris-Levy equation) are

$$\Delta(\sigma_r + \sigma_\theta) = 0 \tag{15}$$

and since it is

$$\sigma_r + \sigma_\theta = \Delta\,\Phi(r,\theta) = \frac{\partial^2\Phi}{\partial r^2} + \frac{1}{r}\frac{\partial\Phi}{\partial r} + \frac{1}{r^2}\frac{\partial^2\Phi}{\partial\theta^2}, \tag{16}$$

where $\Phi(r,\theta)$ is a stress function which satisfies the Maxwell partial differential equation

$$\Delta\,\Delta\,\Phi(r,\theta) = 0. \tag{17}$$

The mechanical stresses components are

$$\sigma_r = \frac{1}{r}\frac{\partial\Phi}{\partial r} + \frac{1}{r^2}\frac{\partial^2\Phi}{\partial\theta^2}, \quad \sigma_\theta = \frac{\partial^2\Phi}{\partial r^2}, \tag{18}$$

$$\tau_{r\theta} = -\frac{\partial}{\partial r}\left(\frac{1}{r}\frac{\partial\Phi}{\partial\theta}\right) = \frac{1}{r^2}\frac{\partial\Phi}{\partial\theta} - \frac{1}{r}\frac{\partial^2\Phi}{\partial r\,\partial\theta}. \tag{19}$$

## 4. Boundary conditions on the crack faces

The boundary conditions on the crack faces (surface sides) are:

For the mode I and the mode II the conditions are defined by means of the mechanical stress components on the crack faces:

1° that the normal stress for the crack surface points for the section with a normal in the circular direction is equal to zero:

$$\sigma_\theta\Big|_{\theta=\pm\pi} = \frac{\partial^2\Phi}{\partial r^2}\Big|_{\theta=\pm\pi} = 0. \tag{20}$$

2° that the shear stress in the circular direction for the surface with a normal in the radial direction for the crack surface points is equal to zero:

$$\tau_{r\theta}\Big|_{\theta=\pm\pi} = -\frac{\partial}{\partial r}\left(\frac{1}{r}\frac{\partial\Phi}{\partial\theta}\right)\Big|_{\theta=\pm\pi} = 0. \tag{21}$$

For the mode III the baundary conditions are defined by means of the mechanical stress components and the electric stress components on the crack surface sides:

1° that the shear stress in the axial direction for the surface with a normal in the circular direction for the crack surface points is equal zero, as well as 2° that the piezoelectric stress circular component at the crack surface points is equal zero:

$$\tau_{\theta z}(r,\pm\pi) = 0, \quad \mathcal{D}_\theta(r,\pm\pi) = 0. \tag{21'))}$$

## 5. Aplication of the complex variable function to the plane deformation state

The relations between the specific deformations and the mechanical stress components are

$$\varepsilon_r = \frac{\partial u}{\partial r} = \frac{1}{c_{11}^2 - c_{12}^2}(c_{11}\sigma_r - c_{12}\sigma_\theta), \tag{22}$$

$$\varepsilon_\theta = \frac{1}{r}\left(\frac{\partial v}{\partial\theta} + u\right) = \frac{1}{c_{11}^2 - c_{12}^2}(c_{11}\sigma_\theta - c_{12}\sigma_r), \tag{23}$$

$$\varepsilon_{r\theta} = \frac{1}{2}\left[\frac{1}{r}\left(\frac{\partial u}{\partial\theta} - v\right) + \frac{\partial v}{\partial r}\right] = \frac{1}{c_{11} - c_{12}}\tau_{r\theta}. \tag{24}$$

If we assume that the volume forces are neglected we have obtained, from the equilibrium conditions, that the stress function $\Phi(r,\theta)$ shold satisfy the Maxwell partial differential equation, i.e., it should be a biharmonic coordinates function and thus it can be represented by means of the complex variable analytical functions

$z = re^{i\theta}$, $i = \sqrt{-1}$. The stress function $\Phi(r,\theta)$ satisfies the partial differential equation

$$\sigma_r + \sigma_\theta = \Delta\,\Phi(r,\theta) = \frac{\partial^2\Phi}{\partial r^2} + \frac{1}{p}\frac{\partial\Phi}{\partial r} + \frac{1}{r^2}\frac{\partial^2\Phi}{\partial\theta^2} = p(r,\theta), \tag{25}$$

where $p(r,\theta)$ is a harmonic function which satisfies the Laplace partial differential equation. Let's introduce the complex function now:

$$f(z) = p(r,\theta) + iq(r,\theta), \tag{26}$$

in which $q(r,\theta)$ is a harmonic function conjugated to the function $p(r,\theta)$ and together with it satisfies the Cauchy-Riemann conditions. The function integral $f(z)$ with respect to the complex variable $z$ is denoted with $\mathcal{F}(z)$ whose real $\mathcal{P}(r,\theta)$ and imaginary $\mathcal{Q}(r,\theta)$ parts are harmonic functions which separately satisfy the Laplace partial differential equation. The first derivative of this complex function $\mathcal{F}(z)$ of the complex variable is

$$\mathcal{F}'(z) = \frac{1}{4}f(z) = \frac{1}{4}[p(r,\theta) + iq(r,\theta)]. \tag{27}$$

By substituting the expresions (18) and (19) into (22) and (23) and having in mind (27) and after integratio with respect to $r$ and $\theta$, we obtain the displacement vector components for the plane deformation state in the form:

$$u(r,\theta) = \frac{c_{11}}{c_{11}^2 - c_{12}^2}\left[4\mathcal{P}(r,\theta)\cos\theta + 4\mathcal{Q}(r,\theta)\sin\theta - \frac{c_{11}+c_{12}}{c_{11}}\frac{\partial\Phi}{\partial r}\right], \tag{28}$$

$$v(r,\theta) = \frac{c_{11}}{c_{11}^2 - c_{12}^2}\left[4\mathcal{Q}(r,\theta)\cos\theta - 4\mathcal{P}(r,\theta)\sin\theta - \frac{c_{11}+c_{12}}{c_{11}}\frac{1}{r}\frac{\partial\Phi}{\partial\theta}\right], \tag{29}$$

where we have left out arbitrary integrating function since we are looking for displacements only for the case of a pure deformation. Let's accept the stress function according to the Ref. [6] in the form

$$\Phi(r,\theta) = \Re e\{\overline{z}\mathcal{F}(z) + \mathcal{X}(z)\} = \frac{1}{2}[\overline{z}\mathcal{F}(z) + \mathcal{X}(z) + z\overline{\mathcal{F}}(\overline{z}) + \overline{\mathcal{X}}(\overline{z})], \tag{30}$$

where dash denotes the conjugated complex parameters whereas the functions $\mathcal{F}(z)$ and $\mathcal{X}(z)$ are the complex variable analytical functions $z$. If we now multiply the displacement component $v(r,\theta)$ expression (29) with an imaginary unit and if we add it to the component displacement $u(r,\theta)$ expression (28) and having in mind the expression (30) we can write down the following relation of the components $u(r,\theta)$ and $v(r,\theta)$ of the displacement vector for the case of the plane deformation and the complex variable analytical functions $\mathcal{F}(z)$ and $\mathcal{X}(z)$ in the form

$$u + iv = \frac{c_{11}}{c_{11}^2 - c_{12}^2}\left\{\frac{3c_{11} - c_{12}}{c_{11}}\mathcal{F}(z) - \frac{c_{11}+c_{12}}{c_{11}}[z\overline{\mathcal{F}}'(\overline{z}) + \overline{\mathcal{X}}'(\overline{z})]\right\}e^{-i\theta}. \tag{31}$$

The relation between the component mechanical stress and the analytical functions $\mathcal{F}(z)$ and $\mathcal{X}(z)$ of the complex variable is (see the References [6] and [11])

$$\sigma_r + \sigma_\theta = 4\Re e\{\mathcal{F}'(z)\} = 2[\mathcal{F}'(z) + \overline{\mathcal{F}}'(\overline{z})], \tag{32}$$

$$\sigma_\theta - \sigma_r + 2i\tau_{r\theta} = 2[\overline{z}\mathcal{F}''(\overline{z}) + \mathcal{X}''(z)]e^{2i\theta}, \tag{33}$$

$$\sigma_r - \sigma_\theta - 2i\tau_{r\theta} = 2[z\overline{\mathcal{F}}''(\overline{z}) + \overline{\mathcal{X}}''(\overline{z})]e^{2i\theta}, \tag{34}$$

$$\sigma_r - i\tau_{r\theta} = \mathcal{F}'(z) + \overline{\mathcal{F}}'(\overline{z}) - [\overline{z}\mathcal{F}''(z) + \overline{\mathcal{X}}''(z)]e^{2i\theta}. \tag{35}$$

Futher application of the complex variable function merhod is in the problem of finding the most proper way of selecting the analytical functions $\mathcal{F}(z)$ and $\mathcal{X}(z)$ of the complex variable for the corresponding crack mode.

## 6. Problem solution for the mode I – crack opening

Let's choose the functions $\mathcal{F}(z)$ and $\mathcal{X}(z)$ of the complex variable in the form of orders:

$$\mathcal{F}(z) = \sum_{n=0}^{\infty} A_n z^{n/2} = A_0 + A_1 z^{1/2} + A_2 z + A_3 z^{3/2} + \cdots, \tag{36}$$

$$\mathcal{X}'(z) = \sum_{n=0}^{\infty} B_n z^{n/2} = B_0 + B_1 z^{1/2} + B_2 z + B_3 z^{3/2} + \cdots, \tag{37}$$

with unknown coefficients $A_n$ and $B_n$ which should be determined from the boundary conditions on the crack surface. By introducing the assumed functions (36) and (37) and their derivatives into the expression (30) for the stress function we obtain it in the form

$$\Phi(r,\theta) = \sum_{n=0}^{\infty} r^{n/2+1}\left(A_n \cos\frac{n-2}{2}\theta + \frac{2B_n}{n+2}\cos\frac{n+2}{2}\theta\right) \tag{38}$$

with unknown coefficients $A_n$ and $B_n$ for which we determine the relation from the boundary conditions (20) and (21) on the crack surface in the form:

$$A_{2n} = -\frac{1}{n+1}B_{2n}, \quad A_{2n+1} = -\frac{2}{2n-1}B_{2n+1}. \tag{39}$$

By introducing the assumed functions $\mathcal{F}(z)$ and $\mathcal{X}(z)$ according to the expressions (36) and (37) in the relation (31) of the displacement vector components and by separating the real and imaginary parts and having in view the coefficients relations

(39) we obtain the following relations for the displacement components:

$$u(r,\theta) = \frac{1}{c_{11}-c_{12}} \sum_{n=0}^{\infty} r^{n/2} \left[ \frac{(6-n)c_{11} - (2+n)c_{12}}{2(c_{11}+c_{12})} A_n \cos\left(\frac{n}{2}-1\right)\theta - \right.$$
$$\left. - B_n \cos\left(\frac{n}{2}+1\right)\theta \right], \tag{40}$$

$$v(r,\theta) = \frac{1}{c_{11}-c_{12}} \sum_{n=0}^{\infty} r^{n/2} \left[ \frac{(6+n)c_{11} - (2-n)c_{12}}{2(c_{11}+c_{12})} A_n \sin\left(\frac{n}{2}-1\right)\theta + \right.$$
$$\left. + B_n \sin\left(\frac{n}{2}+1\right)\theta \right]. \tag{41}$$

The specific deformations – the strain tensor elements are obtained easily by differentiating and by using the previous expressions (40) and (41) and by their introduction into the expressions (22), (23) and (24) so that it is

$$\varepsilon_r(r,\theta) = \frac{1}{c_{11}-c_{12}} \sum_{n=0}^{\infty} \frac{n}{2} r^{n/2-1} \left[ \frac{(6-n)c_{11} - (2+n)c_{12}}{2(c_{11}+c_{12})} A_n \cos\left(\frac{n}{2}-1\right)\theta - \right.$$
$$\left. - B_n \cos\left(\frac{n}{2}+1\right)\theta \right], \tag{42}$$

$$\varepsilon_\theta(r,\theta) = \frac{1}{c_{11}-c_{12}} \sum_{n=0}^{\infty} \frac{n}{2} r^{n/2-1} \left[ \frac{(2+n)c_{11} - (6-n)c_{12}}{2(c_{11}+c_{12})} A_n \cos\left(\frac{n}{2}-1\right)\theta + \right.$$
$$\left. + B_n \cos\left(\frac{n}{2}+1\right)\theta \right], \tag{43}$$

$$\varepsilon_{r\theta}(r,\theta) = \frac{1}{c_{11}-c_{12}} \sum_{n=0}^{\infty} \frac{n}{4} r^{n/2-1} \left[ (n-2) A_n \sin\left(\frac{n}{2}-1\right)\theta + \right.$$
$$\left. + 2B_n \sin\left(\frac{n}{2}+1\right)\theta \right]. \tag{44}$$

The mechanical stress tensor matrix elements are also obtained now by using the expressions from (32) to (35) and by introducing the complex variables into the same assumed functions according to the expressions (36) and (37) and by separating the real from the imaginary part in each of them so that:

* normal stress st the points around the crack tip for the section with a normal in the radial direction with respect to the crack tip

$$\sigma_r(r,\theta) = \frac{1}{2} \sum_{n=0}^{\infty} n r^{n/2-1} \left[ \left(3-\frac{n}{2}\right) A_n \cos\left(\frac{n}{2}-1\right)\theta - B_n \cos\left(\frac{n}{2}+1\right)\theta \right], \tag{45}$$

* normal stress at the points around the crack tip for the section with a normal in the circular direction with respect to the crack tip

$$\sigma_\theta(r,\theta) = \frac{1}{2} \sum_{n=0}^{\infty} n r^{n/2-1} \left[ \left(1+\frac{n}{2}\right) A_n \cos\left(\frac{n}{2}-1\right)\theta + B_n \cos\left(\frac{n}{2}+1\right)\theta \right], \tag{46}$$

* shear stress at the points around the crack tip for the section with a normal in the radial direction with respect to the crack tip, and with the circular direction

$$\tau_{r\theta}(r,\theta) = \frac{1}{2}\sum_{n=0}^{\infty} nr^{n/2-1}\left[\left(\frac{n}{2}-1\right)A_n \sin\left(\frac{n}{2}-1\right)\theta + B_n \sin\left(\frac{n}{2}+1\right)\theta\right], \quad (47)$$

* normal stress at the points around the crack tip for the section with a normal in the axial direction with respect to the crack through its tip

$$\sigma_z(r,\theta) = \frac{2c_{13}}{c_{11}+c_{12}}\sum_{n=0}^{\infty} nr^{n/2-1}A_n \cos\left(\frac{n}{2}-1\right)\theta. \quad (48)$$

The axial component of the piezoelectric stress parallel to the crack front through its tip

$$\mathcal{D}_z(r,\theta) = \frac{2e_{31}}{c_{11}+c_{12}}\sum_{n=0}^{\infty} nr^{n/2-1}A_n \cos\left(\frac{n}{2}-1\right)\theta. \quad (49)$$

## 7. Problem solution for the mode II – crack shear

The function $\mathcal{F}(z)$ and $\mathcal{X}(z)$ of the complex variable can be chosen in the form of the orders

$$\mathcal{F}(z) = i\sum_{n=0}^{\infty} C_n z^{n/2} = iC_0 + iC_1 z^{1/2} + iC_2 z + iC_3 z^{3/2} + \cdots, \quad (50)$$

$$\mathcal{X}'(z) = i\sum_{n=0}^{\infty} D_n z^{n/2} = iD_0 + iD_1 z^{1/2} + iD_2 z + iD_3 z^{3/2} + \cdots. \quad (51)$$

By aplying the procedure similar to the one in the section VI for the case of the mode II crack deformation we determine:

* stress function

$$\Phi(r,\theta) = \sum_{n=0}^{\infty} r^{n/2+1}\left(C_n \sin\frac{2-n}{2}\theta - \frac{2D_n}{n+2}\sin\frac{2+n}{2}\theta\right). \quad (52)$$

By using the boundary conditions (21') from the mode II we determine the relations between unknown constants in the form

$$C_{2n} = \frac{1}{(1-n)(1+n)}D_{2n}, \quad C_{2n+1} = -\frac{2}{2n+3}D_{2n+1}. \quad (53)$$

The displacement vector coordinates for the mode II are now obtained in the form

$$u(r,\theta) = \frac{1}{2(c_{11}-c_{12})}\sum_{n=0}^{\infty} r^{n/2}\left[\frac{(n-6)c_{11}+(2+n)c_{12}}{c_{11}+c_{12}}C_n \sin\left(\frac{n}{2}-1\right)\theta + \right.$$
$$\left. + 2D_n \sin\left(\frac{n}{2}+1\right)\theta\right], \tag{54}$$

$$v(r,\theta) = \frac{1}{2(c_{11}-c_{12})}\sum_{n=0}^{\infty} r^{n/2}\left[\frac{(6+n)c_{11}+(n-2)c_{12}}{c_{11}+c_{12}}C_n \cos\left(\frac{n}{2}-1\right)\theta + \right.$$
$$\left. + 2D_n \cos\left(\frac{n}{2}+1\right)\theta\right]. \tag{55}$$

The line elements dilation and sliding for the mode II are obtained in the form

$$\varepsilon_r(r,\theta) = \frac{1}{2(c_{11}-c_{12})}\sum_{n=0}^{\infty} nr^{n/2-1}\left[\frac{(n-6)c_{11}+(2+n)c_{12}}{2(c_{11}+c_{12})}C_n \sin\left(\frac{n}{2}-1\right)\theta + \right.$$
$$\left. + D_n \sin\left(\frac{n}{2}+1\right)\theta\right], \tag{56}$$

$$\varepsilon_\theta(r,\theta) = \frac{1}{2(c_{11}-c_{12})}\sum_{n=0}^{\infty} nr^{n/2-1}\left[\frac{(6-n)c_{12}-(n+2)c_{11}}{2(c_{11}+c_{12})}C_n \sin\left(\frac{n}{2}-1\right)\theta - \right.$$
$$\left. - D_n \sin\left(\frac{n}{2}+1\right)\theta\right], \tag{57}$$

$$\varepsilon_{r\theta}(r,\theta) = \frac{1}{c_{11}-c_{12}}\sum_{n=0}^{\infty} \frac{n}{4} r^{n/2-1}\left[(n-2)C_n \cos\left(\frac{n}{2}-1\right)\theta + \right.$$
$$\left. + 2D_n \cos\left(\frac{n}{2}+1\right)\theta\right]. \tag{58}$$

The component normal and shear mechanical stresses for the mode II are:

$$\sigma_r(r,\theta) = \frac{1}{2}\sum_{n=0}^{\infty} nr^{n/2-1}\left[\left(\frac{n}{2}-3\right)C_n \sin\left(\frac{n}{2}-1\right)\theta + D_n \sin\left(\frac{n}{2}+1\right)\theta\right], \tag{59}$$

$$\sigma_\theta(r,\theta) = -\frac{1}{4}\sum_{n=0}^{\infty} nr^{n/2-1}\left[(2+n)C_n \sin\left(\frac{n}{2}-1\right)\theta + 2D_n \sin\left(\frac{n}{2}+1\right)\theta\right], \tag{60}$$

$$\tau_{r\theta}(r,\theta) = \frac{1}{2}\sum_{n=0}^{\infty} nr^{n/2-1}\left[\left(\frac{n}{2}-1\right)C_n \cos\left(\frac{n}{2}-1\right)\theta + D_n \cos\left(\frac{n}{2}+1\right)\theta\right], \tag{61}$$

$$\sigma_z(r,\theta) = -\frac{2c_{13}}{c_{11}+c_{12}}\sum_{n=0}^{\infty} nr^{n/2-1}C_n \sin\left(\frac{n}{2}-1\right)\theta. \tag{62}$$

The axial component of the piezoelectric stress parallel to the crack tip front is

$$\mathcal{D}_z(r,\theta) = -\frac{2e_{31}}{c_{11}+c_{12}} \sum_{n=0}^{\infty} n r^{n/2-1} C_n \sin\left(\frac{n}{2}-1\right)\theta. \tag{63}$$

## 8. Mode III – deformation

For the defined mode III – shear of the crack surface out of the referential plane of the crack introduces the assumption that the crack points displacements in the referential plane are equal to zero and that there are only displacements perpendicular to it, that is, in the direction of the crack front, i.e.:

$$u = 0, \quad v = 0, \quad w = w(r,\theta). \tag{64}$$

The relation between the displacement vector components different from zero and the specific deformation tensor components in this case is:

Sliding between the line elements drawn from the point around the crack tip in the radial and axial direction is

$$\varepsilon_{rz} = \frac{1}{2}\frac{\partial w}{\partial r}. \tag{65}$$

Sliding between the line elements drawn from the points around the crack tip in the circular and axial direction is

$$\varepsilon_{\theta z} = \frac{1}{2r}\frac{\partial w}{\partial \theta}, \tag{66}$$

whereas the rest of the relative deformation tensor components are $\varepsilon_{ij} = 0$. By substituting the assumed slidings in the expanded Hooke's Low we obtain the expressions for the mechanical stress tensor components which are diferent from zero:

Shear stress at the point around the crack tip for the section with a normal in the radial direction which is directed in the axial direction:

$$\tau_{rz} = c_{44}\frac{\partial w}{\partial r} - e_{15}E_r. \tag{67}$$

Shear stress at the point around the crack tip for the section with a normal in the circular direction which is directed in the axial direction:

$$\tau_{\theta z} = c_{44}\frac{1}{r}\frac{\partial w}{\partial \theta} - e_{15}E_\theta. \tag{68}$$

By introducing the expression for the assumed slidings into the matrix equation for the piezoelectric stress components we obtain the following expressions for the

piezoelectric stress components in the radial and circular direction at the points around the crack tip:

$$\mathcal{D}_r = e_{15}\frac{\partial w}{\partial r} + \delta_{11}E_r, \quad \mathcal{D}_\theta = e_{15}\frac{1}{r}\frac{1}{\partial w}\partial\theta + \delta_{11}E_\theta, \tag{69}$$

whereas the third component is $\mathcal{D}_z = 0$, since it is $E_z = 0$. If we introduce the expression for electric potential $\Phi_E(r,\theta)$ by means of which we express the electric field components at the points around the crack tip in the form:

$$E_r(r,\theta) = -\frac{\partial \Phi_E}{\partial r}, \quad E_\theta(r,\theta) = -\frac{1}{r}\frac{\partial \Phi_E}{\partial \theta}, \quad E_z = 0. \tag{70}$$

By substituting the previous expressions (15) for the electric field components into the expressions (12), (13) and (14) we obtain the mechanical stress tensor components and the electric field components expressed by means of the component displacement $w(r,\theta)$ and the electric potential $\Phi_E(r,\theta)$ in the form:

The shear mechanical stress components at the points around the crack tip are

$$\tau_{rz} = c_{44}\frac{\partial w}{\partial r} + e_{15}\frac{\partial \Phi_E}{\partial r}, \quad \tau_{\theta z} = c_{44}\frac{1}{r}\frac{\partial w}{\partial \theta} + e_{15}\frac{1}{r}\frac{\partial \Phi_E}{\partial \theta}. \tag{71}$$

The piezoelectric stress components at the points around the crack tip are

$$\mathcal{D}_r = e_{15}\frac{\partial w}{\partial r} - \delta_{11}\frac{\partial \Phi_E}{\partial r}, \quad \mathcal{D}_\theta = e_{15}\frac{1}{r}\frac{\partial w}{\partial \theta} - \delta_{11}\frac{1}{r}\frac{\partial \Phi_E}{\partial \theta}. \tag{72}$$

The equilibrium equations in absance of the volume forces and free electric charges are:

$$\frac{\partial \tau_{rz}}{\partial r} + \frac{1}{r}\frac{\partial \tau_{\theta z}}{\partial \theta} + \frac{\tau_{rz}}{r} = 0, \quad \frac{\partial \mathcal{D}_r}{\partial r} + \frac{1}{r}\frac{\partial \mathcal{D}_\theta}{\partial \theta} + \frac{\mathcal{D}_r}{r} = 0 \tag{73}$$

and are reduced to the following conditions to be satisfied by the component displacement $w(r,\theta)$ and the function $\Phi_E(r,\theta)$ of the electric potential

$$\left(c_{44} + \frac{e_{15}^2}{\delta_{11}}\right)\left(\frac{\partial^2 \Phi_E}{\partial r^2} + \frac{1}{r}\frac{\partial w}{\partial r} + \frac{1}{r^2}\frac{\partial^2 w}{\partial \theta^2}\right) = 0 \Longrightarrow \Delta w = 0, \tag{74}$$

$$\left(\frac{\delta_{11}}{e_{15}}\right)\left(\frac{\partial^2 w}{\partial r^2} + \frac{1}{r}\frac{\partial \Phi_E}{\partial r} + \frac{1}{r^2}\frac{\partial^2 \Phi_E}{\partial \theta^2}\right) = 0 \Longrightarrow \Delta \Phi_E = 0. \tag{75}$$

## 9. Solution for the mode III – shear out of the referential plane by applying the complex variable function

Let's introduce the following analytical functions of the complex variable $z$:

$$\mathcal{W}_1(z) = \sum_{n=0}^{\infty} E_{2n} z^n, \quad \mathcal{W}_2(z) = \sum_{n=0}^{\infty} E_{2n+1} z^{(2n+1)/2}, \tag{76}$$

$$\Phi_1(z) = \sum_{n=0}^{\infty} F_{2n} z^n, \quad \Phi_2(z) = \sum_{n=0}^{\infty} F_{2n+1} z^{(2n+1)/2}, \tag{77}$$

and use them to express the component displacement $w(r,\theta)$ and the function $\Phi_E(r,\theta)$ of the electric potential in the form:

$$w(r,\theta) = \Re e\{\mathcal{W}_1(z) - i\mathcal{W}_2(z)\}, \tag{78}$$

$$\Phi(r,\theta) = \Re e\{\Phi_1(z) - i\Phi_2(z)\}. \tag{79}$$

By separating the real parts of the defined functions of the complex variables in the previous expressions we obtain: The coordinates of the displacement vector of the points around the crack tip

$$w(r,\theta) = \sum_{n=0}^{\infty} \left( E_{2n} r^n \cos n\theta + E_{2n+1} r^{(2n+1)/2} \sin \frac{2n+1}{2}\theta \right). \tag{80}$$

The electric potential at the points around the crack tip is

$$\Phi(r,\theta) = \sum_{n=0}^{\infty} \left( F_{2n} r^n \cos n\theta + F_{2n+1} r^{(2n+1)/2} \sin \frac{2n+1}{2}\theta \right). \tag{80}$$

The strain tensor matrix elements at the points around the crack tip are:

* sliding between the line elements drawn from the point around the crack tip in the radial direction with respect to the crack tip and in the axial direction of the crack front

$$\varepsilon_{rz}(r,\theta) = \frac{1}{4} \sum_{n=0}^{\infty} \left[ 2nE_{2n} r^{n-1} \cos n\theta + (2n+1) E_{2n+1} r^{(2n-1)/2} \sin \frac{2n+1}{2}\theta \right], \tag{82}$$

* sliding between the line elements drawn from the point around the crack tip in the circular direction with respect to the crack tip and in the axial direction of the crack front

$$\varepsilon_{\theta z}(r,\theta) = \frac{1}{4} \sum_{n=0}^{\infty} \left[ -2nE_{2n} r^{n-1} \sin n\theta + (2n+1) E_{2n+1} r^{(2n-1)/2} \cos \frac{2n+1}{2}\theta \right]. \tag{83}$$

The mechanical stress tensor matrix elements are all equal to zero except for the two of them which represent shear component stresses:

* shear stress at the point around the crack tip for the section with a normal in the radial direction with respect to the crack tip directed to the crack front direction

$$\tau_{rz}(r,\theta) = \frac{1}{2} \sum_{n=0}^{\infty} \left[ 2n \left( c_{44} E_{2n} + e_{15} F_{2n} \right) r^{n-1} \cos n\theta + \right.$$

$$\left. + (2n+1) \left( c_{44} E_{2n+1} + e_{15} F_{2n+1} \right) r^{(2n-1)/2} \sin \frac{2n+1}{2}\theta \right], \tag{84}$$

* shear stress at the point around the crack tip for the section with a normal in the circular direction with respect to the crack tip direction in the crack front direction

$$\tau_{\theta z}(r,\theta) = \frac{1}{2}\sum_{n=0}^{\infty}\Big[-2n\Big(c_{44}E_{2n} + e_{15}F_{2n}\Big)r^{n-1}\sin n\theta + \\ + (2n+1)\Big(c_{44}E_{2n+1} + e_{15}F_{2n+1}\Big)r^{(2n-1)/2}\cos\frac{2n+1}{2}\theta\Big]. \tag{85}$$

The piezoelectric stress components are:

* the piezoelectric stress component at the point around the crack tip in the radial direction with respect to it:

$$\mathcal{D}_r(r,\theta) = \frac{1}{2}\sum_{n=0}^{\infty}\Big[2n\Big(e_{15}E_{2n} - \delta_{11}F_{2n}\Big)r^{n-1}\cos n\theta + \\ + (2n+1)\Big(e_{15}E_{2n+1} - \delta_{11}F_{2n+1}\Big)r^{(2n-1)/2}\sin\frac{2n+1}{2}\theta\Big], \tag{86}$$

* the piezoelectric stress component at the point around the crack tip in the circular direction with respect to it:

$$\mathcal{D}_\theta(r,\theta) = \frac{1}{2}\sum_{n=0}^{\infty}\Big[-2n\Big(e_{15}E_{2n} - \delta_{11}F_{2n}\Big)r^{n-1}\sin n\theta \\ + (2n+1)\Big(e_{15}E_{2n+1} - \delta 11F_{2n+1}\Big)r^{(2n-1)/2}\cos\frac{2n+1}{2}\theta\Big]. \tag{87}$$

The electric field components at the points around the crack tip:

* the electric field components at the points around the crack tip in the radial direction with respect to it:

$$E_r(r,\theta) = -\frac{1}{2}\sum_{n=0}^{\infty}\Big[2nF_{2n}r^{n-1}\cos n\theta + (2n+1)F_{2n+1}r^{(2n-1)/2}\sin\frac{2n+1}{2}\theta\Big], \tag{88}$$

* the electric field components at the points around the crack tip in the circular direction with respect to it:

$$E_\theta(r,\theta) = -\frac{1}{2}\sum_{n=0}^{\infty}\Big[2nF_{2n}r^{n-1}\sin n\theta + (2n+1)F_{2n+1}r^{(2n-1)/2}\cos\frac{2n+1}{2}\theta\Big]. \tag{89}$$

## 10. Numerical applications with graphical representations

In order to draw conclusions about the crack behaviour in the given piezoelectric material we shall observe VIBRIT 420 with density $\rho = 7600\,kg/m^3$. This

material belongs to a hexagonal crystal system of the crystal class $6_{mm}(C_{6V})$ and the following numerical data can be written for it:

The elasticity tensor matrix:

$$(\mathcal{C}) = \begin{pmatrix} c_{11} & c_{12} & c_{13} & 0 & 0 & 0 \\ c_{12} & c_{11} & c_{13} & 0 & 0 & 0 \\ c_{13} & c_{13} & c_{33} & 0 & 0 & 0 \\ 0 & 0 & 0 & c_{44} & 0 & 0 \\ 0 & 0 & 0 & 0 & c_{44} & 0 \\ 0 & 0 & 0 & 0 & 0 & \frac{c_{11}-c_{12}}{2} \end{pmatrix}$$

$$= \begin{pmatrix} 14.9 & 10.1 & 9.8 & 0 & 0 & 0 \\ 10.1 & 14.9 & 9.8 & 0 & 0 & 0 \\ 9.8 & 9.8 & 14.3 & 0 & 0 & 0 \\ 0 & 0 & 0 & 2.2 & 0 & 0 \\ 0 & 0 & 0 & 0 & 2.2 & 0 \\ 0 & 0 & 0 & 0 & 0 & 2.4 \end{pmatrix} 10^{10} \left[\frac{N}{m^2}\right]. \tag{90}$$

The piezoconstant tensor matrix:

$$\begin{pmatrix} 0 & 0 & e_{31} \\ 0 & 0 & e_{31} \\ 0 & 0 & e_{33} \\ 0 & e_{15} & 0 \\ e_{15} & 0 & 0 \\ 0 & 0 & 0 \end{pmatrix} = \begin{pmatrix} 0 & 0 & -5.4 \\ 0 & 0 & -5.4 \\ 0 & 0 & 13.5 \\ 0 & 11.7 & 0 \\ 11.7 & 0 & 0 \\ 0 & 0 & 0 \end{pmatrix} \left[\frac{C}{m^2}\right]. \tag{91}$$

The dielectric constant tensor matrix at a given deformation:

$$(\mathcal{D}) = \begin{pmatrix} \delta_{11} & 0 & 0 \\ 0 & \delta_{11} & 0 \\ 0 & 0 & \delta_{33} \end{pmatrix} = \begin{pmatrix} 8 & 0 & 0 \\ 0 & 8 & 0 \\ 0 & 0 & 7.2 \end{pmatrix} 10^{-9} \left[\frac{F}{m}\right]. \tag{92}$$

The numerical analysis of the mechanical and electric stresses state and of the strain state and of the deformation state of the given piezoelectric material around the crack tip on the basis of the derived formulae for each mode separately we shall perform by changing the polar angle $\theta$ within the range $\pm\pi$ at the constant radius $r = const.$ ($r = 10\,mm$) and by changing the radius at the constant polar angle $\theta = const.$ In the second case the angle $\theta$ is chosen so that $\theta = 0, \pm\pi$, by which we have comprised the two neighbouring crack surfaces and the direction, that is, the section immediately under the crack tip. This enable direct view of the effect of the mechanical and electric stress tensor components upon the propagation process of the crack according to the linear elastic fracture mechanics theory.

Since the aim is to present a graphical representation of the distribution of the electromechanical properties of a piesoelectric material in the crack tip zone and since it is $r \to 0$ then we can preserve the members which considerably affect this distribution. Therefore, we keep only the members having the indices 1 and for

this case we perform the data proceeding according to the analytical expressions we have determined and we form up the graphics shown in the sketches from No. 5 to 38.

The given sketches show the reduced diagrams in the zones around the crack tip of the component mechanical stresses, of the component piezoelectric stresses, of the component specific deformations and the displacement vectors components for the mode I (sketches No. 5 to 14 and the sketch No. 25) and for the mode II (sketches from No. 15 to 24 and the sketch No. 26) and for the mode III (sketches from No. 27 to 38) of the carck.

## 11. Conclusion

In attempt to reach a better understending of the piezoelectric material fracture mechanics in the presence of the mechanical and electrical stresses we have observed a semi-infinite crack which is found as a defect in an imaginary infinite piezoelectric material. The analytical expressions for the mechanical stress state and strain state as well as for electric field state and dielectric stress in a piezoelectric material at the points around the crack tip we have approximated by the trigonometric functions by using the method of the complex variable function and by applying the linear elasticity theory with an assumption about the plane deformation forming, that is, about the deformation space state depending on the assumed deformation mode. The complex variable analytical functions are assumed in the form of the graded Laurent orders with infinite number of members which are used to construct the stress function for the case of the first two modes and for third mode the component displacement and electric potencial are constructed.

On the basis of the shown sketches for the mode I we can derive the following conclusions: On the crack surface $\theta = \pm\pi$ the extreme value maximum is obtained only by the component displacement $u$ perpendicular to the crack surface whereas all the other components of the mechanical stress and deformation as well as the piezoelectric stress component have the extreme values – minima.

Moreover, on the basis of the shown sketches for the mode II we derive the following conclusions: On the crack surface $\theta = \pm\pi$ the extreme value – maximum is obtained by the normal stress $\sigma_r$ for the surface with a normal in the radial direction (sketch N0. 15), the normal stress $\sigma_z$ for the section with a normal in the axial direction (sketch No. 17), the piezoelectric stress component $\mathcal{D}_z$ in the axial direction (sketch No. 21), strain $\varepsilon_r$ of the line element drawn from the crack point in the circular in the radial direction (sketch No. 19), strain $\varepsilon_\theta$ of the line element drawn from the crack point in the circular direction (sketch No. 20), the component displacement $u$ of the crack points (sketch No. 23); the extreme value – minimum – is obtained by the normal stress $\sigma_\theta$ for the surface with a normal in the circular direction (sketch No. 16), the shear stress $\tau_{r\theta}$ (sketch No. 8), and the sliding $\varepsilon_{r\theta}$ of the line elements drawn from the crack point in the radial and circular direction as well as the displacement vector component perpendicular to the crack surface (sketch No. 12).

The components having maximum at the points on the crack surface for the mode I and the mode II crack deformation considerably affect the crack propagation (growth) in a piezoelectric material.

The analysis and the comparsion of the obtained graphical representations of the electromechanical state in a piezoelectric material at the points around the crack tip show that both the components of the displacement vector of the points for the given approximation are directly proportional to the square root of the polar coordinate $r$ which presents a distance between the observed point from the crack tip. By observing the reduced diagram of the component $v$ of the displacement vector which is perpendicular to the surface crack for the mode I of the crack deformation we see that it grows along with the point movment away from the crack tip whereas the component tangential to the crack surface is equal to zero at all its points.

For the mode II of the crack deformation we conclude that the displacement vector components in the tangential direction on the crack surface at the points of one crack surface increase the others decline as they approach the crack tip.

The mechanical and piezoelectric components at stresses for both the modes in the given approximation are inversely proportional to the square root of the distance of the point from the crack tip and it they have singular values. The same conclusion stands for the tensor strain components as well.

On the basis of the shown sketches for the mode III we can derive the following conclusions: On the crack surface $\theta = \pm\pi$ the extreme value – maximum is obtained by:

* shear stress $\tau_{rz}(r, \pm\pi)$ for a section with a normal in the radial direction which is directed towards the crack point (sketch No. 27);
* radial component $\mathcal{D}_r(r, \pm\pi)$ of the piezoelectric stress (sketch No. 29);
* relativ deformation $\varepsilon_{rz}(r, \pm\pi)$ sliding between the line elements in the radial and axial direction lying in the crack plane (sketch No. 31);
* radial component $E_r(r, \pm\pi)$ of the electric field (sketch No. 33);
* component $w(r, \pm\pi)$ of the displacement vector in the crack front direction (sketch No. 35);
* electric potential $\Phi_E(r, \pm\pi)$ (sketch No. 36).

The influence of the maximum of the previously mentioned parameters of the electromechanical state of a piezoelectric material on the mode III of the crack is considerable since it considerably effects the crack propagation. Also, on the crack surface $\theta = \pm\pi$ the extreme value – maximum – is obtained by:

* shear stress $\tau_{\theta z}(r, \pm\pi)$ for a section with a normal in the circular direction, which is directed towards the crack front (sketch No. 28);
* circular component $\mathcal{D}_\theta(r, \pm\pi)$ of the piezoelectric stress (sketch No. 30);
* relativ deformation $\varepsilon_{\theta z}(r, \pm\pi)$ sliding between the line elements in the circular and axial direction lying the plane perpendicular to the crack plane (sketch No. 32);
* circular component $E_\theta(r, \pm\pi)$ of the electric field (sketch No. 34).

The parameters of the electromechanical state of a piezoelectric material which are minimal on the crack surface do not affect considerably the crack propagation.

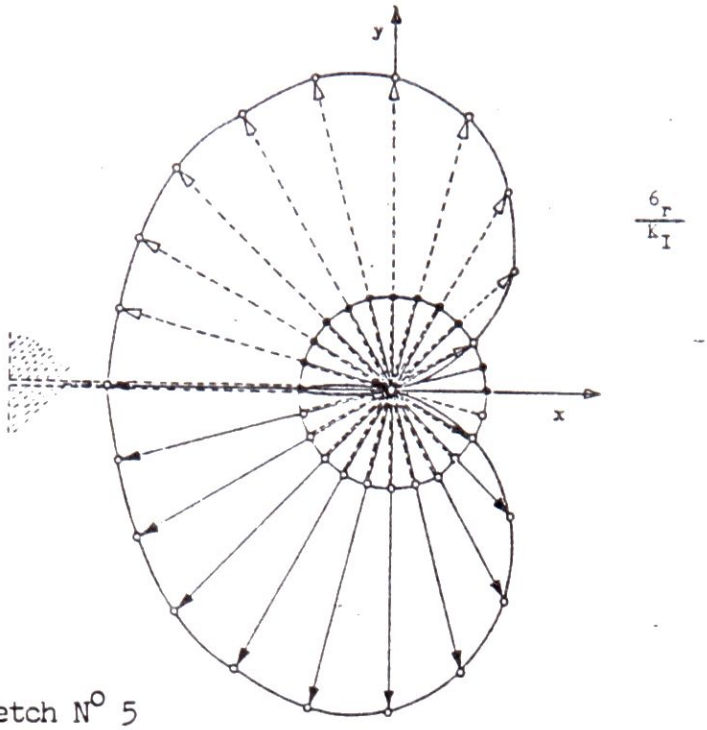


Sketch N° 5

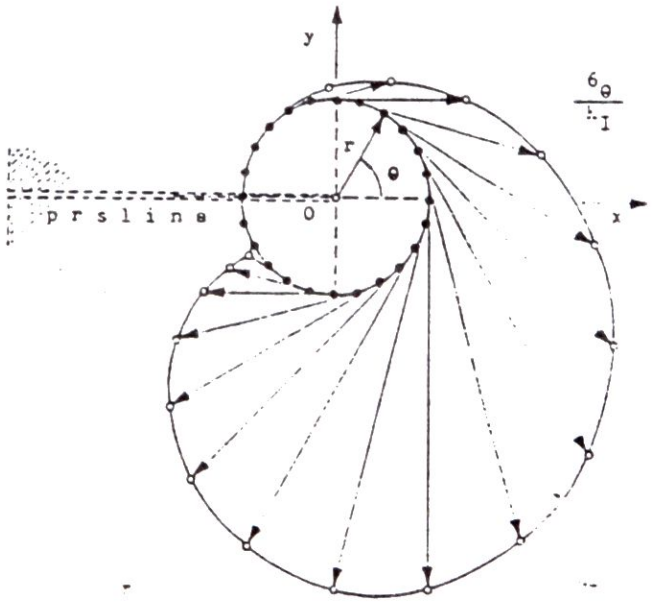


Sketch N° 6

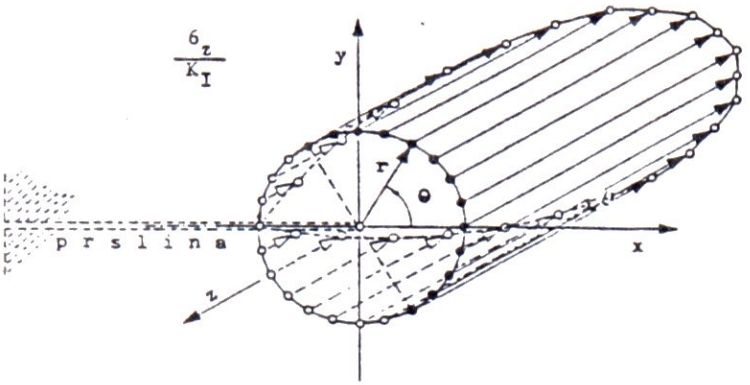


Sketch N° 7

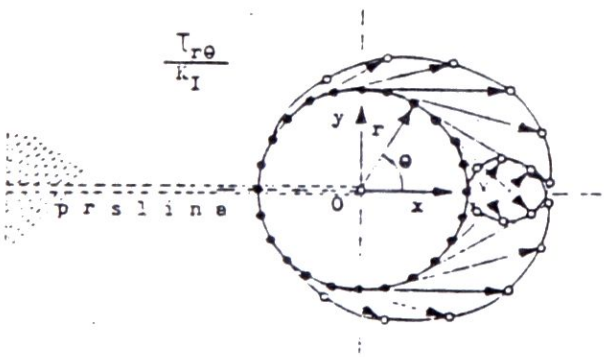


Sketch N° 8

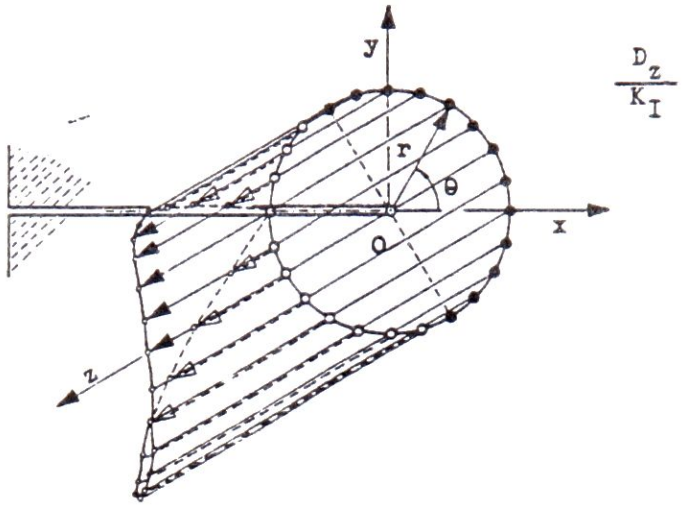


Sketch N$^{o}$ 9

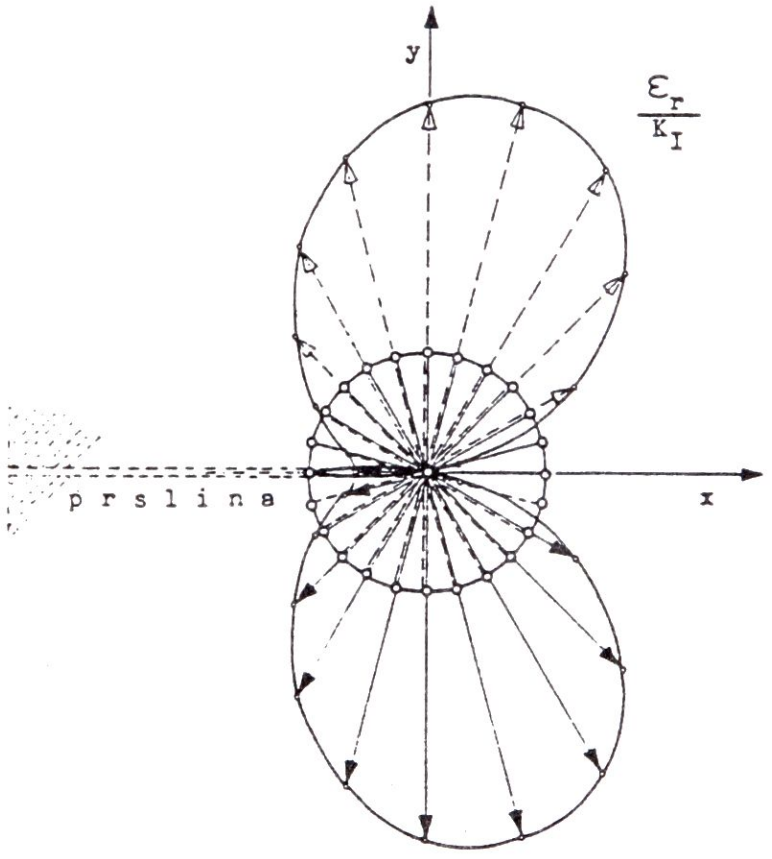


Sketch N$^{o}$ 10

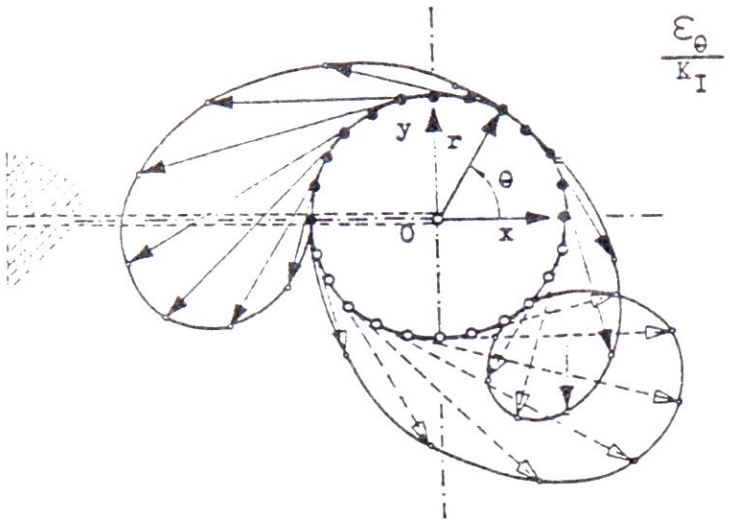


Sketch N° 11

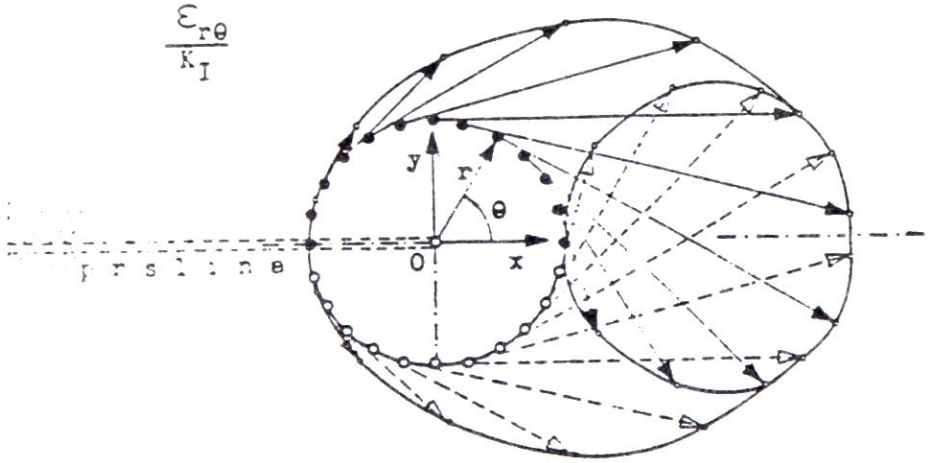


Sketch N° 12

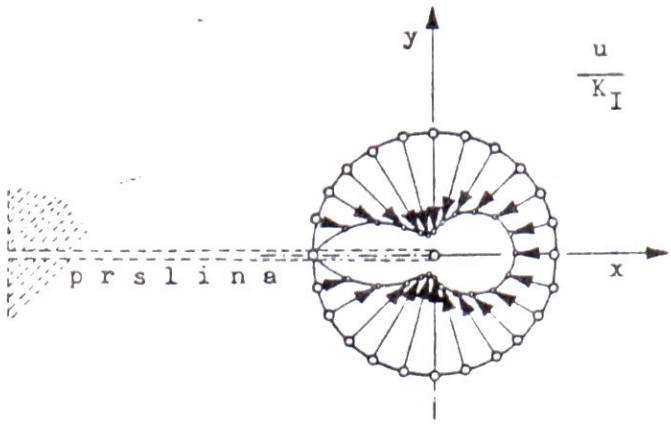


Sketch N° 13

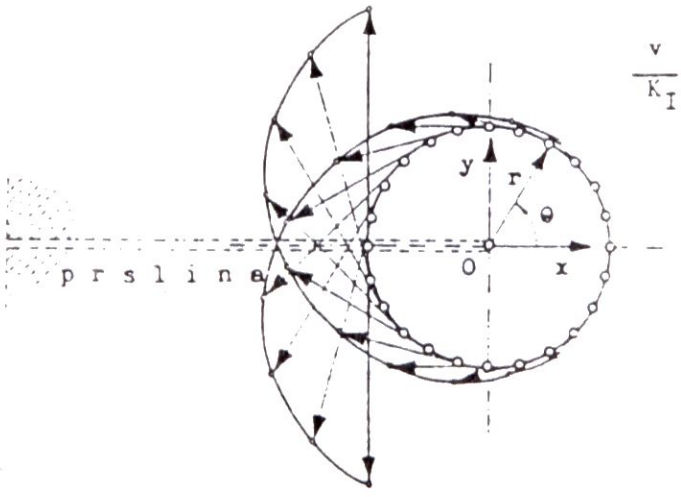


Sketch N° 14

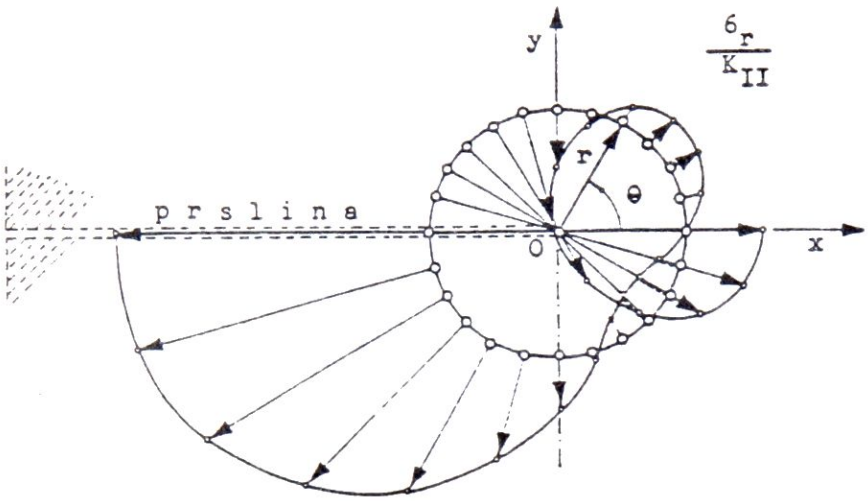


Sketch N° 15

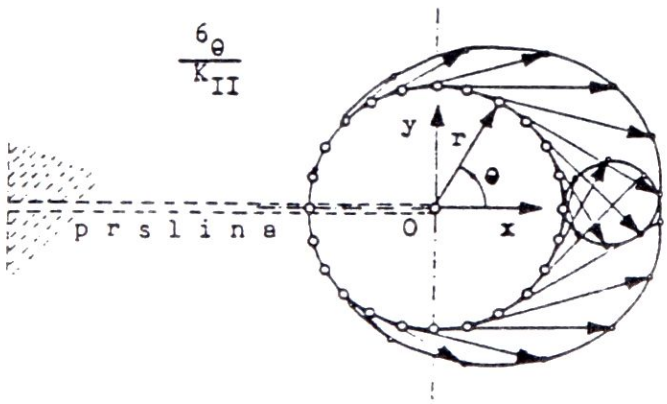


Sketch N° 16

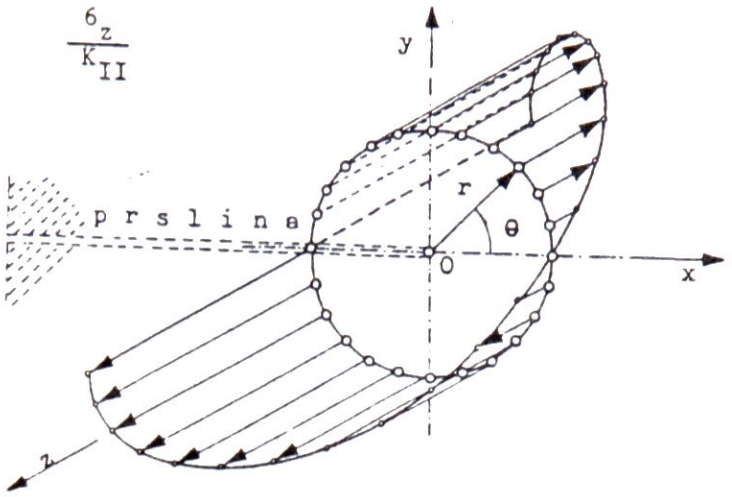


Sketch N$^{O}$ 17

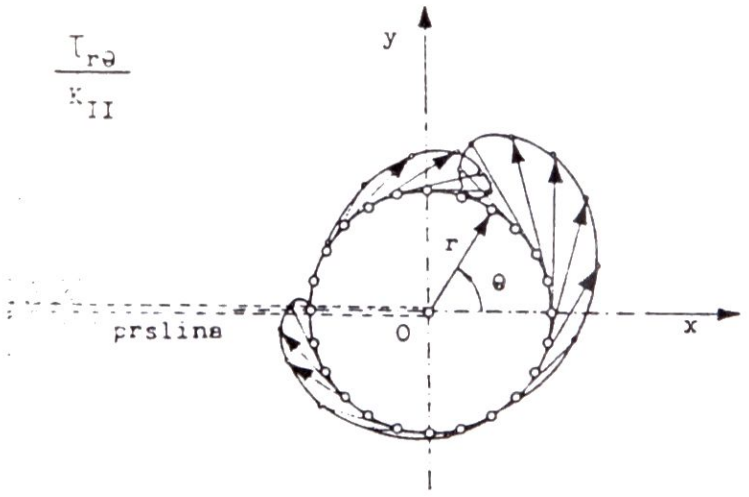


Sketch N$^{O}$ 18

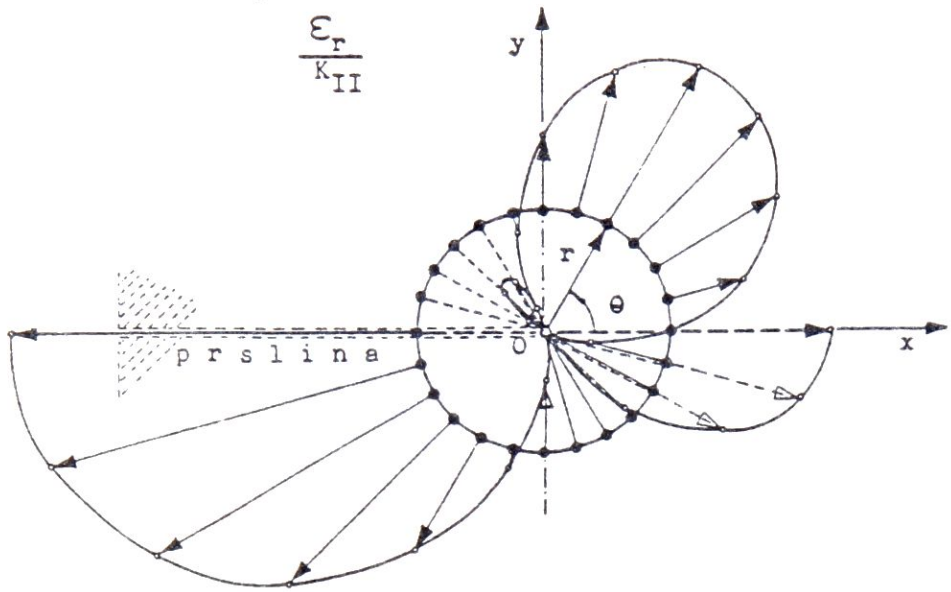


Sketch N° 19

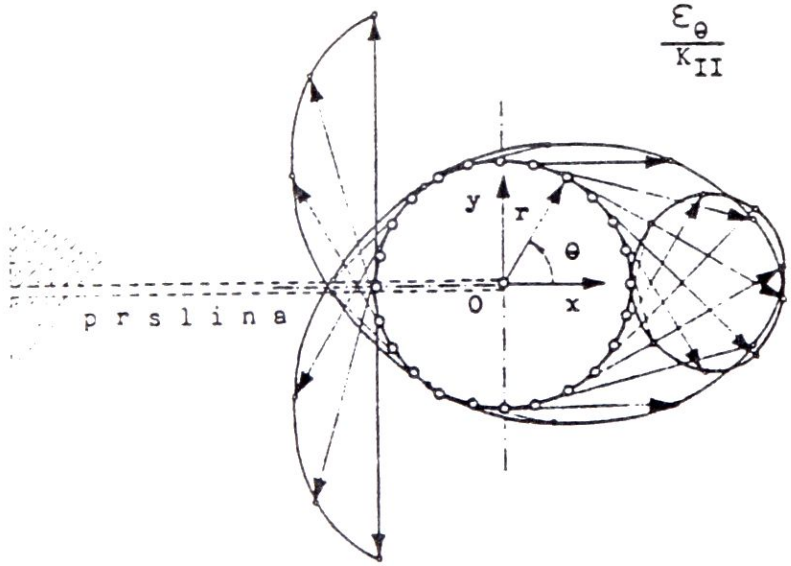


Sketch N° 20

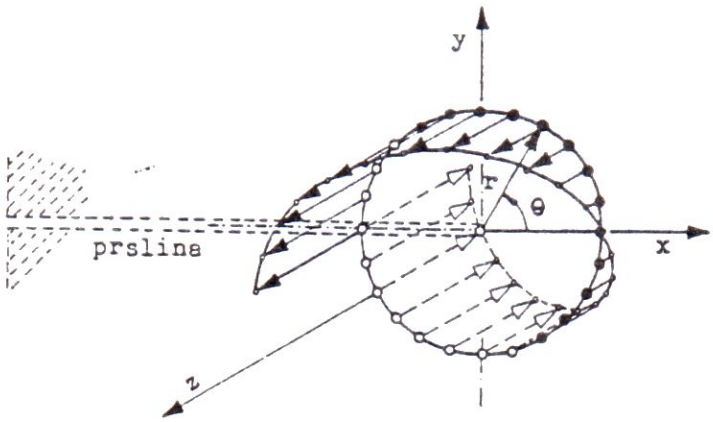


Sketch N$^{O}$ 21

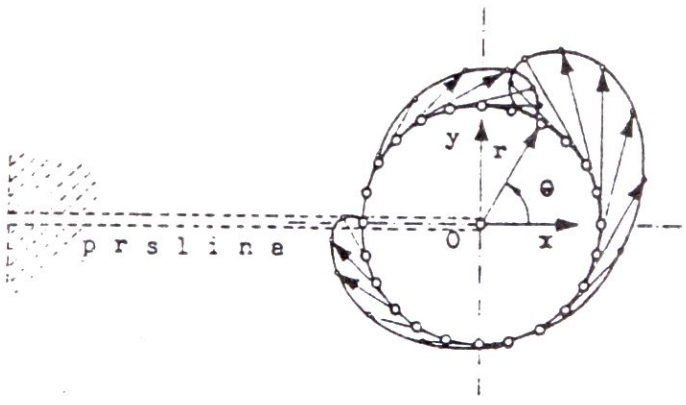


Sketch N$^{O}$ 22

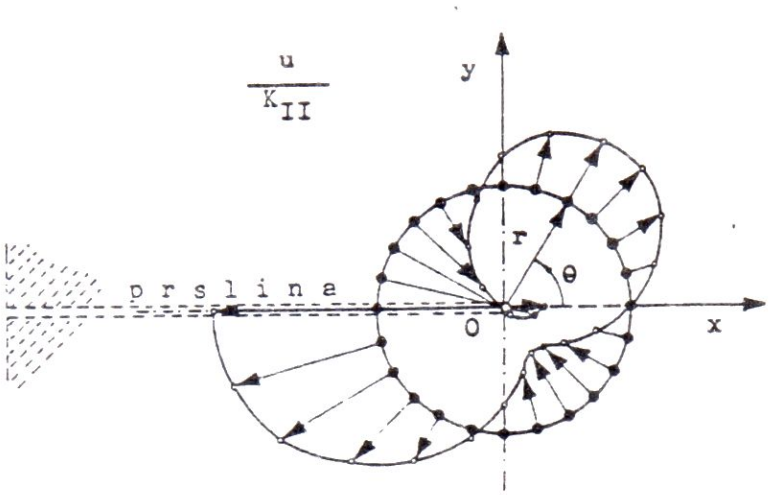


Sketch N° 23

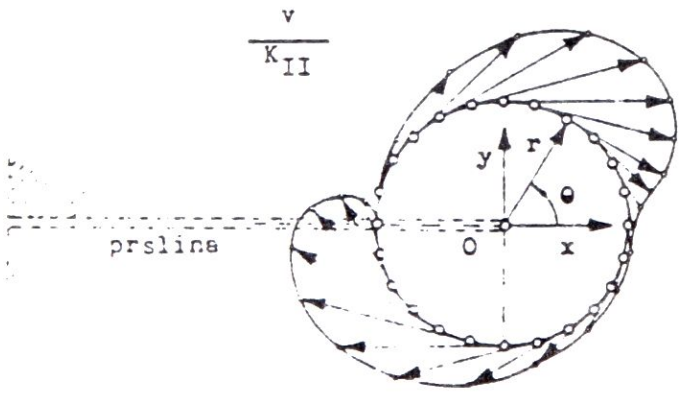


Sketch N° 24

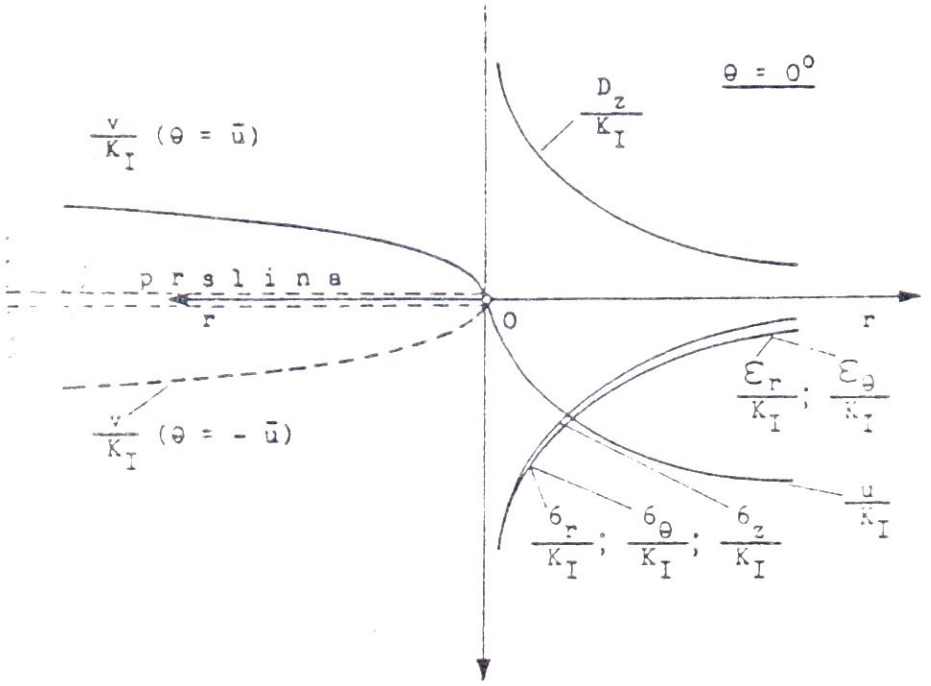


Sketch N° 25

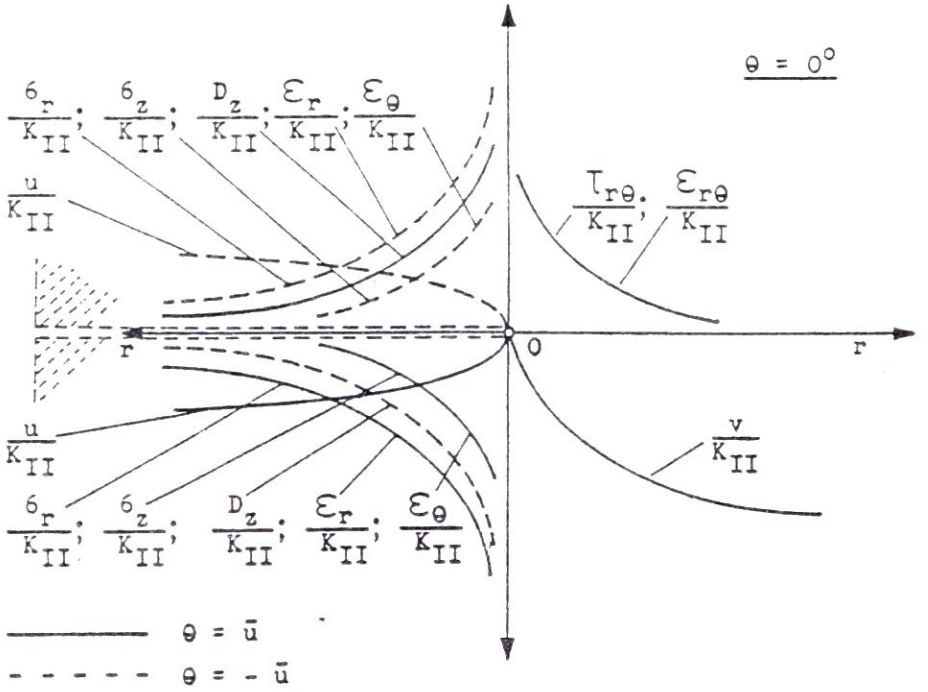


Sketch N° 26

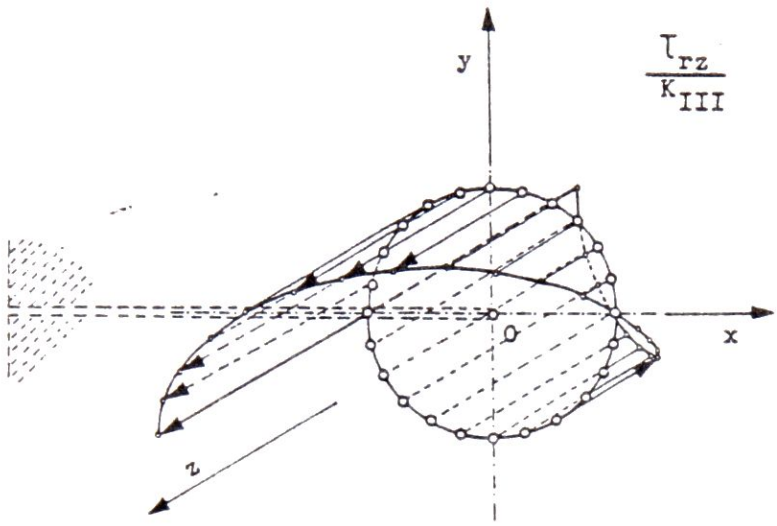


Sketch N° 27

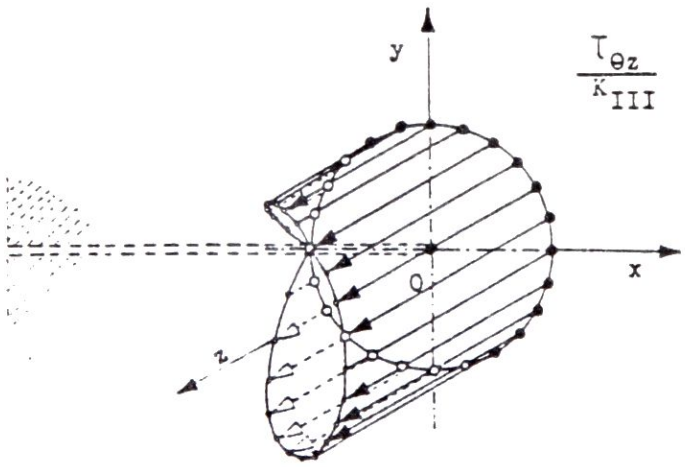


Sketch N° 28

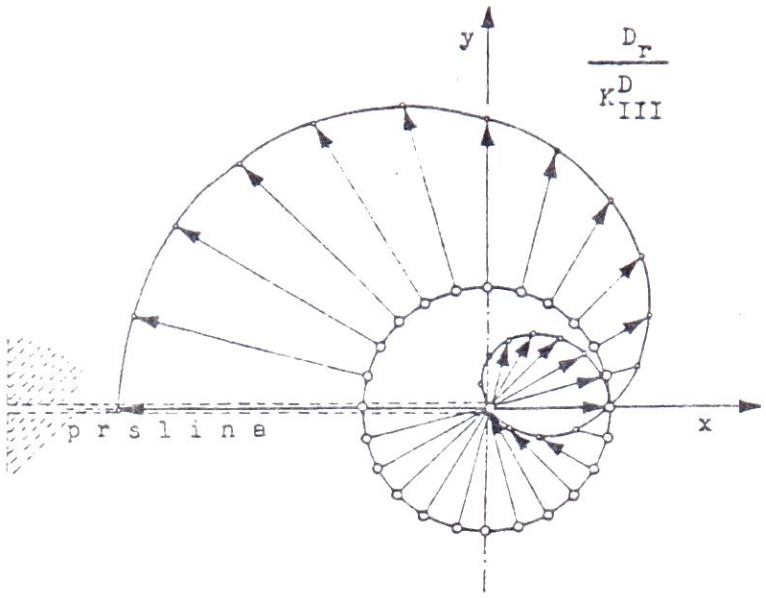


Sketch N$^{O}$ 29

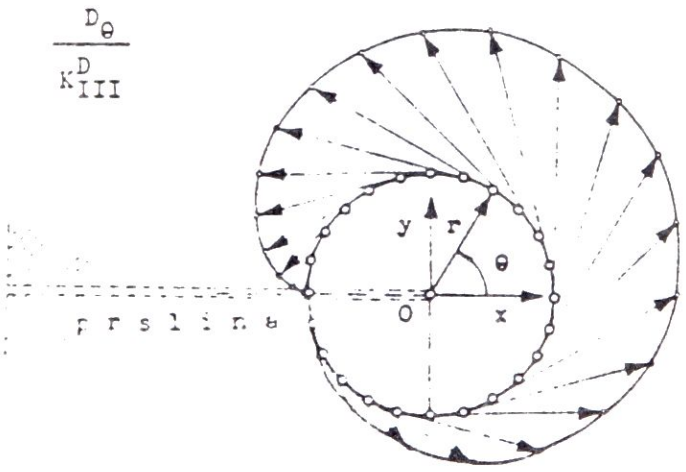


Sketch N$^{O}$ 30

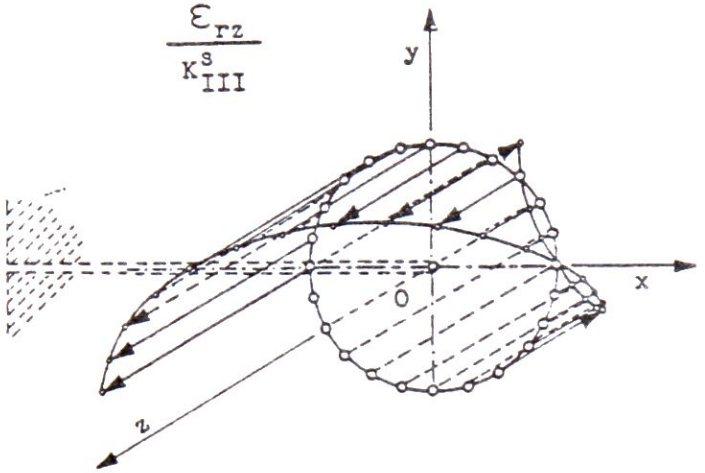


Sketch N° 31

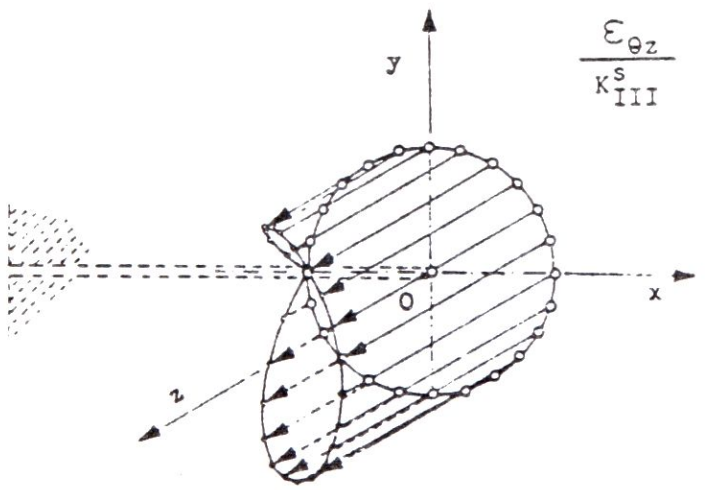


Sketch N° 32

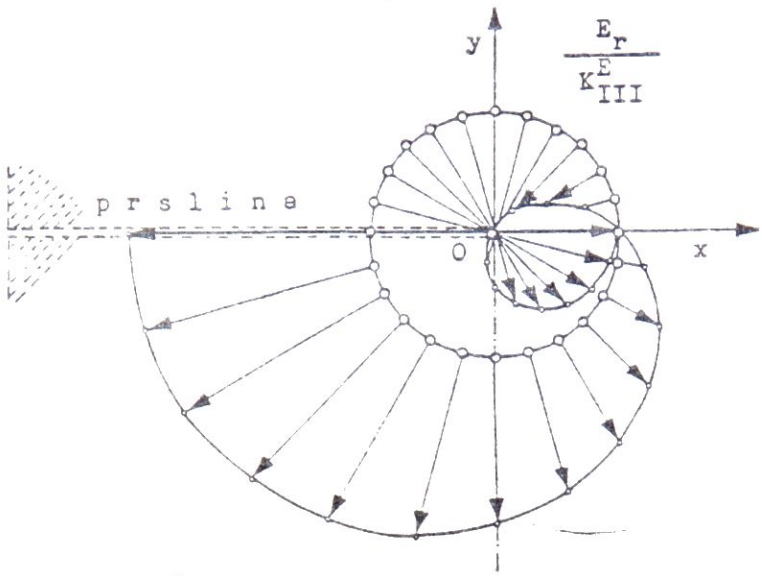


Sketch N$^{O}$ 33

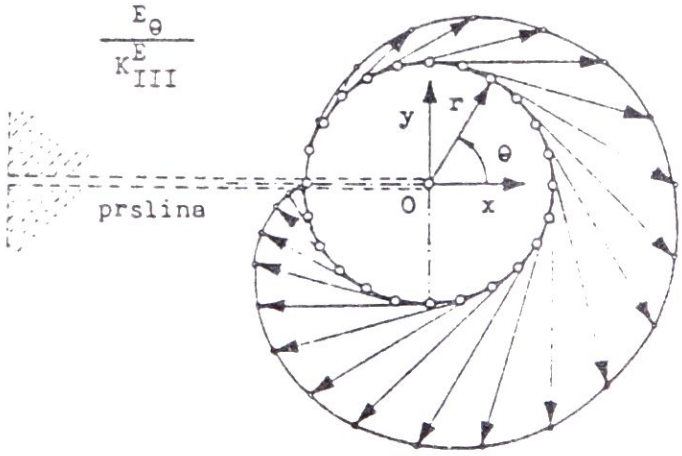


Sketch N$^{O}$ 34

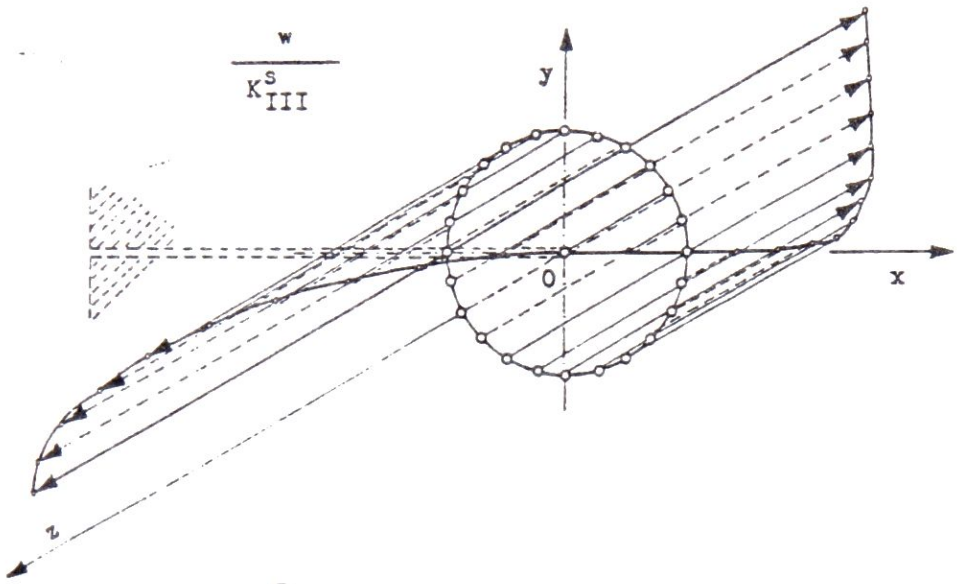


Sketch N° 35

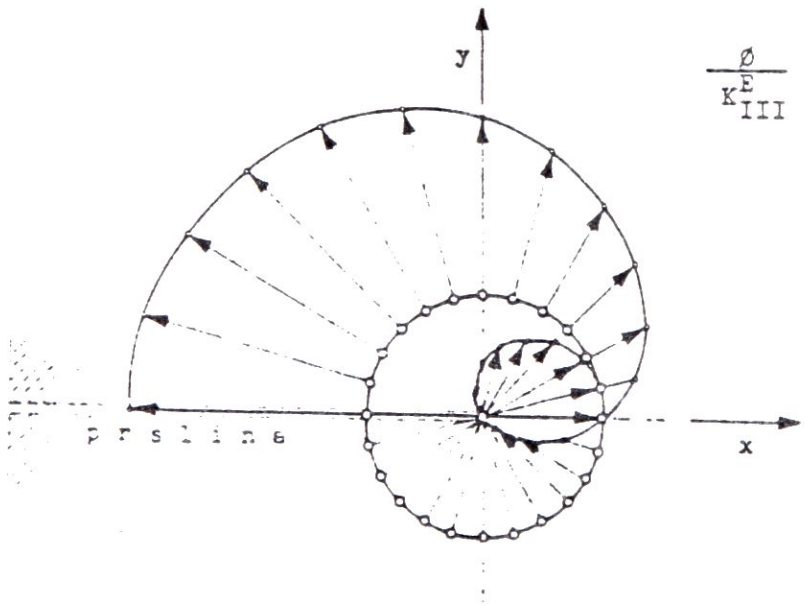


Sketch N° 36

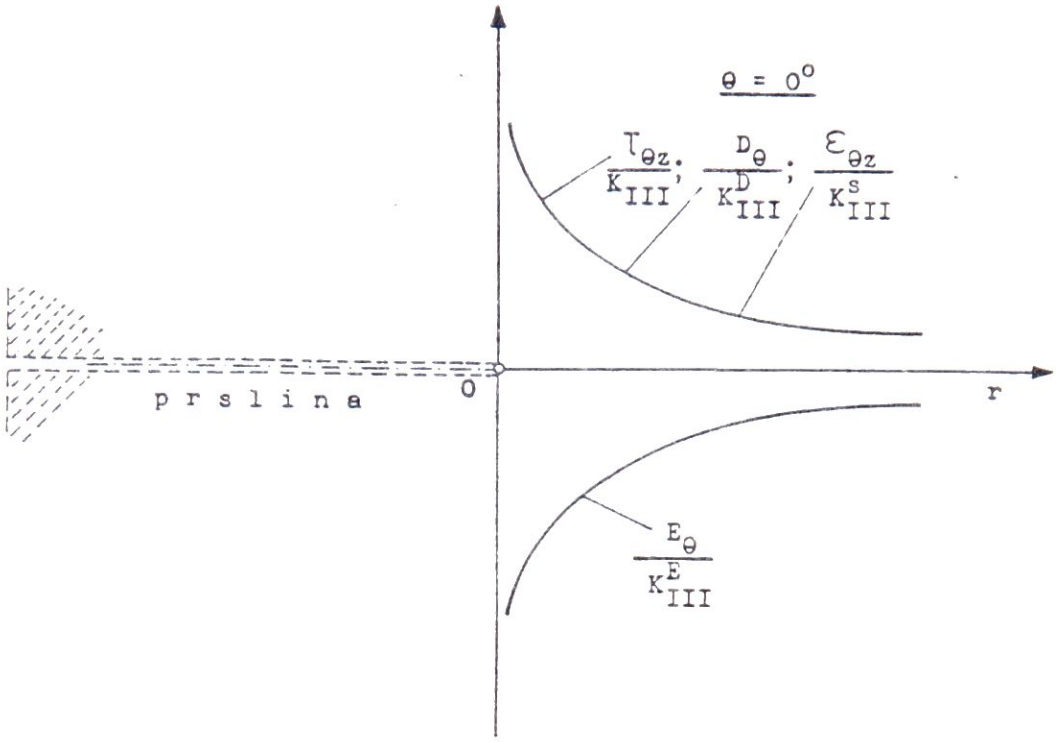


Sketch N° 37

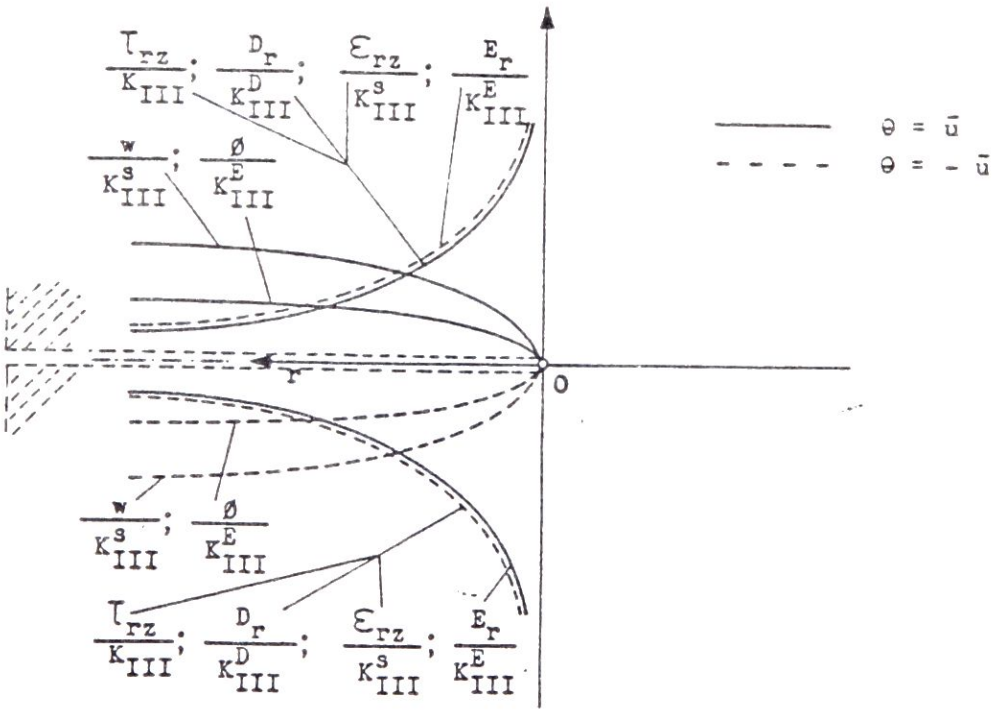


Sketch N° 38

The analysis and the comparsion of the obtained graphical representations of the electromechanical state in a piezoelectric material at the points around the crack tip for the mode III we see that the component displacement $w(r,\theta)$ and the electric potential $\Phi_E(r,\theta)$ at the points around the crack tip for the given approximation are proportional to the square root of the point distance from the crack tip.

To repeat, in our analyses, we have introduced the assumption about the linear elastic fracture mechanics which assumes limitless elasticity which never occurs in practice. In any deformation no matter how small it is a plastic zone forms around the crack tip immediately which makes the stress value finite. If the nonlinear zone around the crack tip is so small that it is all contained in the electric stress field, then its effect upon the stress distribution at a certain distance from the tip (front) of the crack can be comprised by the stress intensity factors $\Re_I$ (for mode I), $\Re_{II}$ (for mode II) and $\Re_{III}$ (for mode III) which represent the measure of the stress intensity immediately in front of the crack tip.

All this points to the conclusion that the very appearance of a crack in the stressed piezoelectric material, if it happens, can bring about redistribution and stress concentration as well as the appearance of singular state at the very crack tip. The very crack tip as a singular point represents a spot of the greatest stress concentration and the piezoelectric material is at place the most sensitive to later fracture appearance.

The shown procedure for determining the electromechanical state of a piezoelectric material as well as the graphical representations represent, in our opinion, a modest but original contribution to the knowledge of the crack impact upon the material fracture as well as to the possibilities of the application of the complex variable functions to the problem solution in the field of the fracture theory.

**Acknowledgement.** This research was suported by Science Fund of Serbia, grant number 0402 through Institute of Mathematics SANU, Belgrade. (This paper was reported at the Mechanical Engineering Faculty, University of Nish, on April 8th, 1992, and at the Department of the Mathematical Institute Serbian Academy of Arts and Science, Belgrade, on April 9th, 1992.)

## REFERENCES

[1] Deeg, W. F., *The Analysis of Dislocation, Crack and Inclusion Problems in Piezielectric Solids*, Ph.D. Thesis, Stanford University (1980).

[2] Frieman, S. W., *Mechanical Behaviour of Ferroelectric Ceramics*, IEEE Sixth International Symp. on Application of Ferroelectric, pp. 367-373 (1986).

[3] Grinchenko, V. T., Ulitko, A. F. and Chulga, N. A., *Mehanika svyzanih polye v elementah konstrukcii - ELEKTROUPRUGOST*, Naukova Dumka, Kiev (1989).

[4] Harrison, W. B., McHenry, K. D. and Koepke, B. G., *Monolitic Multilayer Piezoelectric Ceramic Transducers*, IEEE Sixth International Symp. on Application of Ferroelectric, pp. 265-272 (1986).

[5] Hartranft, R. J., *The use Eigenfunction Expansion in the General Solution of Threedimensional Crack Problems*, J. Math. Mech. 19 (1969), pp. 123-138.

[6] Hedrih (Stevanović), K., *Izabrana poglavlja Teorije elastičnosti*, Mašinski fakultet Niš (1988).

[7] Hedrih (Stevanović), K., Prokić, M. i Radmanović, M., *Promena sopstevnih učestanosti longitudinalnih oscilacija sendvič štapa sa piezokeramičkim pločicama i uticaj mehaničke pobude na stabilnost električne impedance*, A-14, Zbornik radova 18 Jugoslovenskog kongresa teorijske i primenjene mehanike, Vrnjačka Banja (1988).

[8] Hedrih (Stevanović), K. i Mitić S., *Ravno naprezanje kružno-prstenaste ploče*, C1-1, Zbornik radova 18 Jugoslovenskog kongresa teorijske i primenjene mehanike, Vrnjačka Banja (1988).

[9] Hedrih (Stevanović) K. i Mitić, S., *Analiza stanja napona i stanja deformacija revno-napregnute kružno-prstenaste ploče, primenom funkcije kompleksne promenljive*, "Tehnika"-"Mašinstvo" br. 3-4 (1990), Beograd.

[10] Hedrih (Stevanović), K., Jecić, S. i Jovanović, D., *Glavni naponi u tačkama konture eliptično-prstenaste ravno napregnute ploče*, "Tehnika"-"Mašinstvo", br. 11-12 (1990), Beograd.

[11] Hedrih (Stevanović), K. i Jovanović, D., *Primena funkcije kompleksne promenljive i konformnog preslikavanja za određivanje eliptičko-hiperboličkih koordinata tenzora napona ravno napregnutih ploča*, Zbornik radova Kongresa Teorijske i primenjene mehanike Jugoslovenskog društva za mehaniku, Ohrid (1990).

[12] Hedrih (Stevanović), K. i Perić, Lj., *Stanje napona i stanje deformacija u piezoelektričnom materijalu u okolini vrha prsline za slučaj ravne deformacije*, rad pripremljen za štampu.

[13] Hedrih (Stevanović), K. i Perić, Lj., *Stanje napona i stanje deformacija u piezoelektričnom materijalu u okolini vrha prsline za slučaj smicanja izvan referentne ravni*, rad pripremljen za štampu.

[14] Murakami, Y., *Stress Intensity Factors Handbook*, Vol. 1,2, Pergamon Press (1987).

[15] "Irsid Otua", *La rupture des aciers - 2 - La Mécanique de la rupture*, Institute de Rechrches de la Sidérugie - "IRSID" - Saint Germainne - Laye, Office Technique pour l'Utilisation de L'Acier - "OTUA" - Neuilly-sur Seine.

[16] Jaffe, B., Cook, W. R. and Jaffe, H., *Piezoelectric Ceramics*, New York, Academic Press (1971).

[17] Parton, V. Z., *Fracture Mechanics of Piezoelectric Materials*, Acta Astronautica, 3 (1976), pp. 671-683.

[18] Pak, Y. E., *Crack Extension Force in a Piezoelectric Material*, Advanced Development Report 20-11-87.1., Grumman Aerosspace Corporation (1987).

[19] Pak, Y. E., *Force on a Piezoelectric Screw Dislocation*, Journal of Applied Mechanics, Vol 57/863 (1990).

[20] Perić, Lj., *Prostorna analiza uticaja prskotine na lom pizoelektričnog materijala*, seminarski rad, Mašinski fakultet, Niš (1990).

[21] Pisarenko, G. G., Chusko, V. M. and Kovalev, S. P., *Anysotopy of fracture touhness of piezoelectric ceramics*, J. Am. Ceram. Soc. 68 (1985), 259-265.

[22] Ratvani, M., *Lom u uslovima ravne deformacije i ravnog stanja napona i značaj oblika epruvete*, prevod sa engleskog, Uvod u mehaniku loma i konstruisanje sa sigurnošću loma, TMF Beograd (1980) str. 55-69.

[23] Sedmak, S., *Razvoj i osnovne definicije mehanike loma*, Uvod u mehaniku loma i konstruisanje sa sigurnošću loma, TMF Beograd (1980), str. 1-27.

[24] Sosa, A. H. and Pak, Y. E., *Three-dimensional eigenfunction analysis of a crack in a piezoelectric material, 1 - Mechanical Engineering and Mechanics, Drexel University, Philadelphia, PA 19-104, U.S.A.; 2 - Grumman Corporate Research Center, Bethpage, NY 11714, U.S.A., 12 Dec. (1988).*

[25] Tada, H., *The stress analysis of crack handbok*, Del Research Corporation, Hellertown (1973).

[26] Tiersten, H. F., *Linear Piezoelectric Plate Vibrations*, Plenum Press, New York (1969).

[27] Šumarac, D. and Krajčinović, D., *A simple solution of a crack reiforced by bonds*, Eng. Fracture Mechanics, vol. 33, No. 6 (1989), p. 949.

## ПРИМЕНЕНИЕ ФУНКЦИИ КОМПЛЕКСНОЙ ПЕРЕМЕННОЙ В ПРОСТРАНСТВЕННОМ АНАЛИЗЕ СОСТОЯНИЯ НАПРЯЖЕНИЙ И СОСТОЯНИЯ ДЕФОРМАЦИИ У ПЬЕЗОЭЛЕКТРИЧЕСКОМ МАТЕРИАЛЕ С ТРЕЩИНОЙ

В настоящей работе сделан пространственный анализ состояния напряжения и состояния деформации в пьезоэлектрическом материале в точках окрестности вершины трещины для случая деформирования растяжением, попречным сдвигом и продольным сдвигом, применяя теорию линейно-упругой механики разрушения и линейную теорию упругости. Использован метод аналитических функций комплексиной переменой в полярных координатах. Введены функциии механического напряжения и электрическог потенциала. Сделанный нами анализ показывает характерическое поведение координат тензора механического напряжения, пьезоэлектрического напряжения и тензора относительной деформации и электрического поля. У этих составляющих электромеханического состояния материала особые точки в вершине трещины. Эта окрестность вершины прещины является зоной концентрации напряжения и самой чувствительной областю на более поздное появление разрушения материала.

В работе также сделаны вычислительный анализ полученных аналитических результатов для всех трех случаев деформирования трещины: Мод I, мод II и мод III и соответствующие графические представления распределения параметров электромеханического состояния в окрестности вершины трещины пьезоэлектрического материала.

## PRIMENA FUNKCIJA KOMPLEKSNE PROMENLJIVE NA REŠAVANJU PROBLEMA PRSLINE U PIEZOELEKTRIČNOM MATERIJALU

U radu je izvršena prostorna analiza stanja napona i stanja deformacija u piezoelektričnom materijalu u tačkama okoline vrha prsline za slučaj smicanja materijala po površi prsline u i izvan referentne ravni, primenom teorije Linearne elastične mehanike loma (LEML) i linearne teorije elastičnosti. Korišćena je metoda analitičkih funkcija kompleksne promenljive interpretirana pomoću polarno-cilindričnih koordinata. Uvedena je naponska funkcija i funkcija električnog potencijala koje su izražene polarnim koordinatama i trigonometrijskim redovima. Izvedena analiza pokazuje karakteristično ponašanje koordinata tenzora mehaničkog napona, piezoelektričnog napona i relativnih deformacija. Komponente analiziranih tenzora stanja piezoelektričnog materijala imaju singularne vrednosti u vrhu polubeskonačne prsline. Okolina vrha prsline i vrh prsline kao singularna tačka stanja napona i stanja deformacije se javlja kao oblast koncentracije napona i kao najosetljivija zona na kasniju pojavu loma. Takođe je izvršena numerička analiza dobijenih analitičkih rezultata za sva tri moda deformacije prsline i dati su odgovarajući grafički prikazi uticaja stanja napona i stanja deformacije ne proces propagacije u piezoelektričnom materijalu.

Prof. dr. Katica (Stevanović) Hedrih
Mechanical Engineering Faculty University of Niš
18000 Niš
ul. Vojvode Tankosića 3/22
Yugoslavia, Serbia
tel-fax (018) 41-663